SAND2015-8876C

Exceptional service in the national interest

Sandia National Laboratories

Developing a physically-based tantalum strength model: Integrating fundamental concepts with macroscale models

Hojun Lim[1], Corbett Battaile[1], Jay Carroll[2], Justin Brown[3], Thomas Buchheit[2], Fadi Abdeljawad[1], Steve Owen[4], Christopher Weinberger[4], Brad Boyce[2]

[1]Computational Materials & Data Science, [2]Materials Mechanics & Tribology,
[3]Dynamic Material Properties, [4]Simulation Modeling Sciences,
Sandia National Laboratories

[4]Department of Mechanical Engineering & Mechanics,
Drexel University

U.S. DEPARTMENT OF ENERGY

NNSA National Nuclear Security Administration

Sandia National Laboratories is a multi-program laboratory managed and operated by Sandia Corporation, a wholly owned subsidiary of Lockheed Martin Corporation, for the U.S. Department of Energy's National Nuclear Security Administration under contract DE-AC04-94AL85000.

Multi-scale Approach

Multi-scale simulation & experiments to understand & predict material's reliability

Atomic scale phenomena	Single crystal behavior	Microstructural effects	Material Performance
10^{-9} m	10^{-6} m	10^{-3} m	10^{0} m

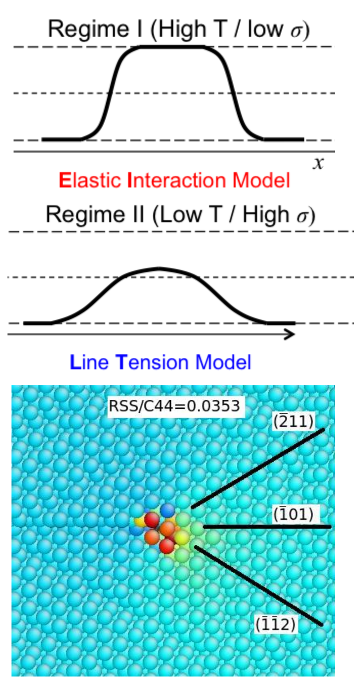

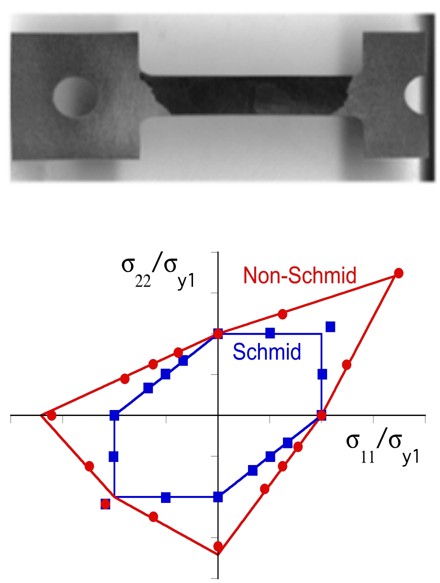

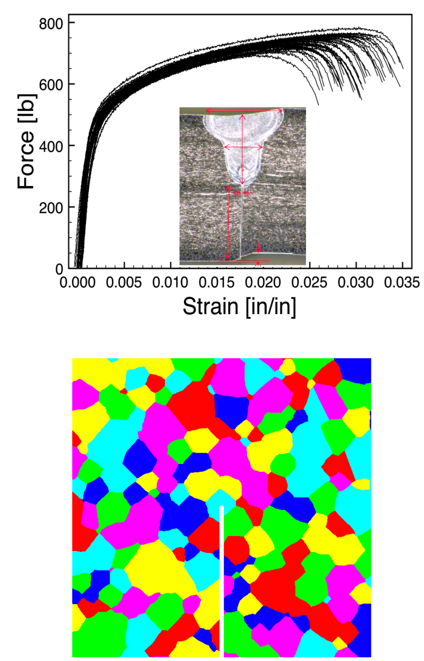

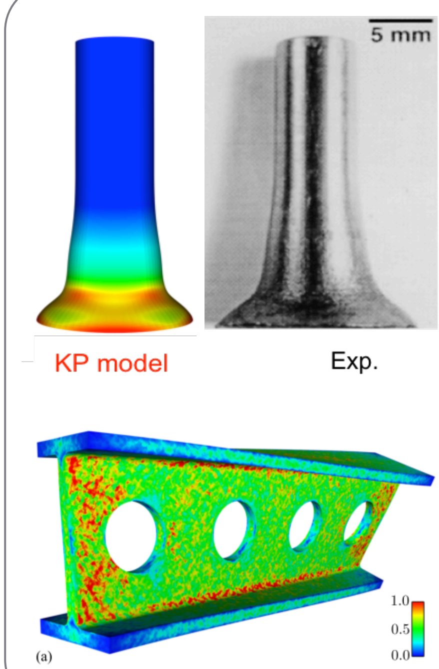

Outline

- Introduction
- Ta strength model incorporating effects of T, $\dot{\epsilon}$ and P
- Experimental Validation of CP-FE Simulations
- Grain-scale Microstructural Variability
- Polycrystalline modeling using phase field grain growth model
- Summary

Ta strength model incorporating effects of temperature, strain rate and pressure

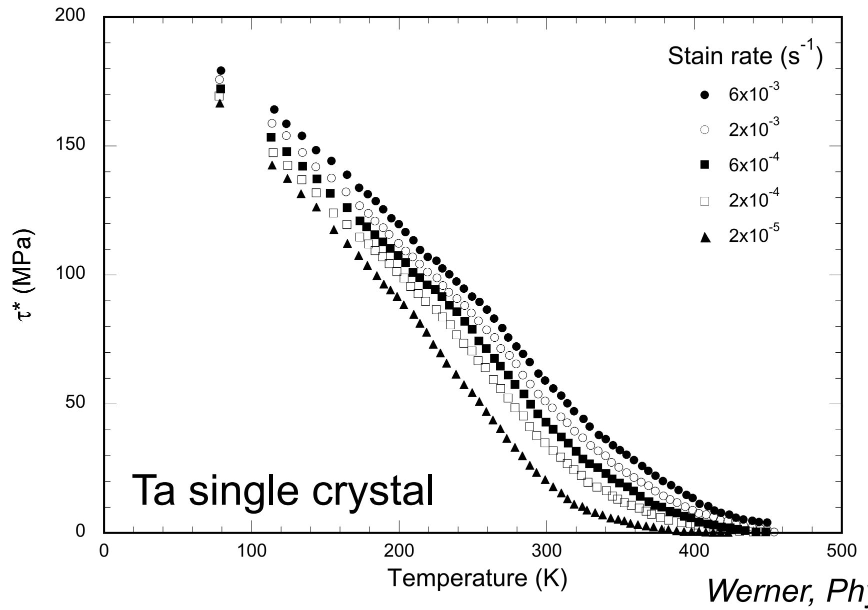

Werner, Phys. Stat. Sol. (a) (1987)

- Lim, H., Battaile, C. C., Carroll, J. D., Boyce, B. L., Weinberger, C. R., 2015. "A physically based model of temperature and strain rate dependent yield in BCC metals: Implementation into crystal plasticity", J. Mech. Phys. Sol., 74, 80–96.

Dislocation Kink-Pair Theory

$$\tau(T,\dot{\gamma}) = \underbrace{\tau^*(T,\dot{\gamma})}_{\text{Thermal}} + \underbrace{\tau_{obs}}_{\text{Athermal}}$$

In FCC metals, $\tau^* \approx 0$

In BCC metals, $\tau^* >> 0 \qquad (T << T_c)$

Peierls barrier and thermal activation of dislocations

Low T / High σ

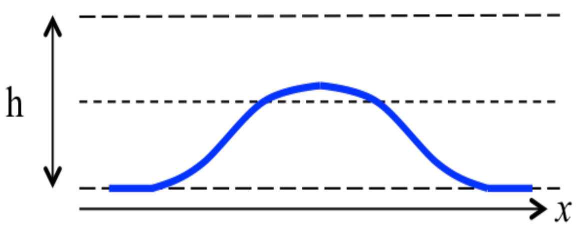

Line Tension Model

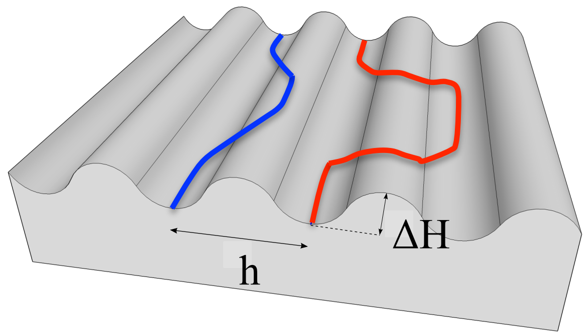

High T / low σ

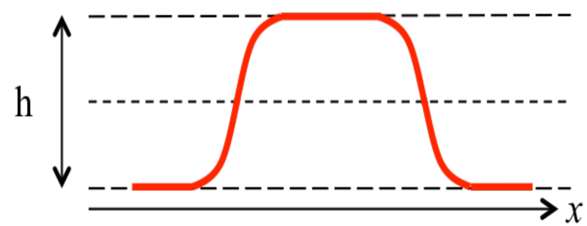

Elastic Interaction Model

$$\tau^*_{LT}(T,\dot{\gamma}) = \tau^0_{LT}\left[1-\left(\frac{k_B T}{2H_k}\ln\left(\frac{\dot{\gamma}_0}{\dot{\gamma}}\right)\right)^{1/2}\right]$$

(Antiparabolic Peierls potential)

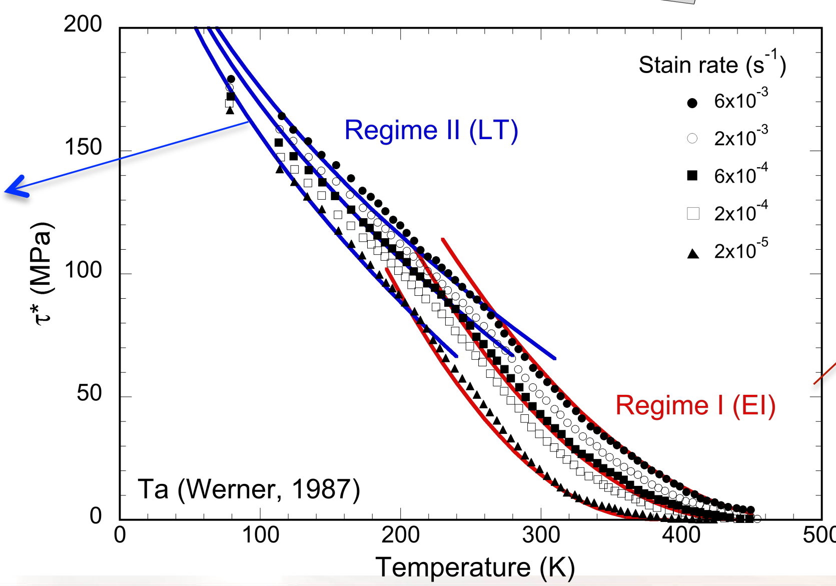

$$\tau^*_{EI}(T,\dot{\gamma}) = \tau^0_{EI}\left[1-\frac{k_B T}{2H_k}\ln\left(\frac{\dot{\gamma}_0}{\dot{\gamma}}\right)\right]^2$$

Pressure Dependence

- Pressure dependent shear modulus

$$\mu(T,P) = \mu_0 - \frac{\partial \mu}{\partial T}(T-300) + \alpha_1 P + \alpha_2 P^2$$

$$\frac{\partial \mu}{\partial T} = 0.009\ GPa/K$$
$$\alpha_1 = 7.99 \times 10^{-1}\quad GPa^{-1}$$
$$\alpha_2 = 2.13 \times 10^{-3}\quad GPa^{-2}$$

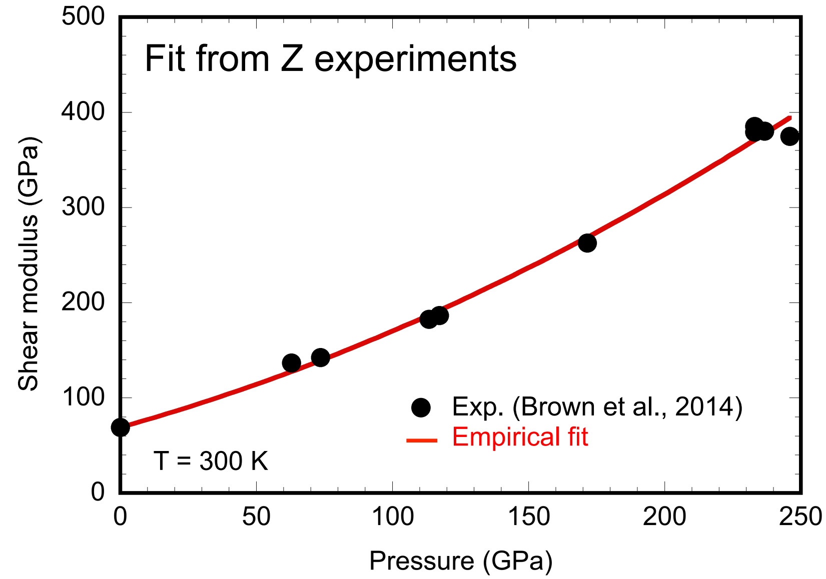

- Pressure dependent yield strength

$$\tau = \min\left(\tau^*_{EI}, \tau^*_{LT}\right) + \tau_{obs}$$

$$\tau^*_{EI} = \frac{\mu}{\mu_0}\tau^0_{EI}\left[1 - \left(\frac{\mu_0 k_B T \ln(\dot{\gamma}_0/\dot{\gamma})}{\mu(2H^0_k)}\right)\right]^2$$

$$\tau^*_{LT} = \frac{\mu}{\mu_0}\tau^0_{LT}\left[1 - \left(\frac{\mu_0 k_B T \ln(\dot{\gamma}_0/\dot{\gamma})}{\mu(2H^0_k)}\right)^{1/2}\right]$$

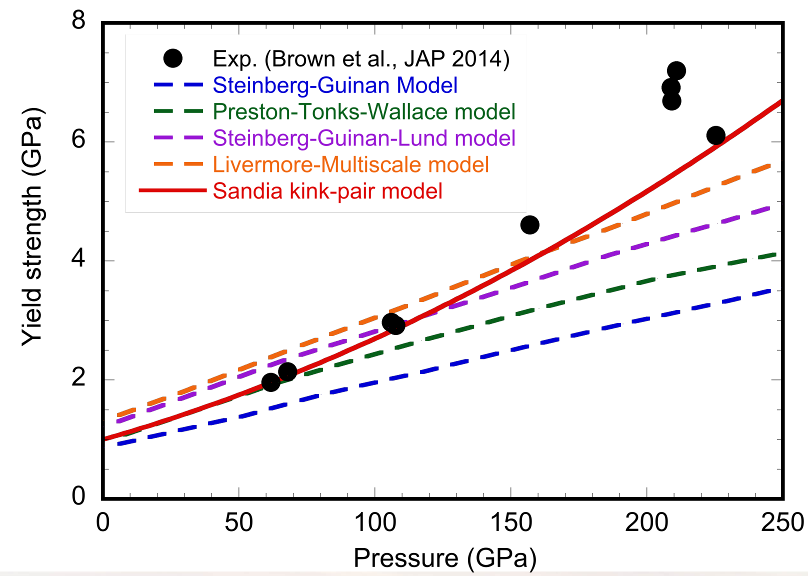

BCC Crystal Plasticity Framework

- FEM code developed at Sandia National Laboratories (JAS-3D)
- 24 {110}<111> slip systems
- Slip rate: $\dot{\gamma}^{\alpha} = \dot{\gamma}_0^{\alpha}\left(\frac{\tau^{\alpha}}{g^{\alpha}}\right)^{1/m}$ (Hutchinson, 1976)
- Slip resistance: $g^{\alpha} = \min\left(\tau_{EI}^{*\alpha}, \tau_{LT}^{*\alpha}\right) + \tau_{obs}^{\alpha}$
  - τ_{obs}^{α} → Obstacle stress
  - $\min\left(\tau_{EI}^{*\alpha}, \tau_{LT}^{*\alpha}\right)$ → Lattice friction
- Obstacle stress: $\tau_{obs}^{\alpha} = A\mu b\sqrt{\sum_{\beta=1}^{NS}\rho^{\beta}}$ (Taylor, 1934)

$$\dot{\rho}^{\alpha} = \left(\kappa_1\sqrt{\sum_{\beta=1}^{NS}\rho^{\beta}} - \kappa_2\rho^{\alpha}\right)\cdot\left|\dot{\gamma}^{\alpha}\right|$$ (Kocks, 1976)

Temperature and Strain Rate Dependence

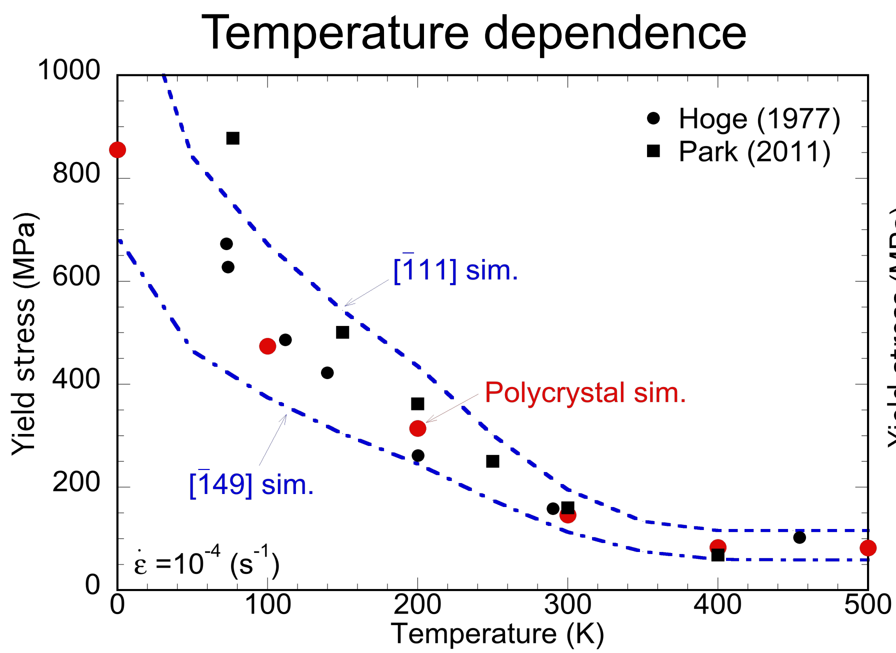

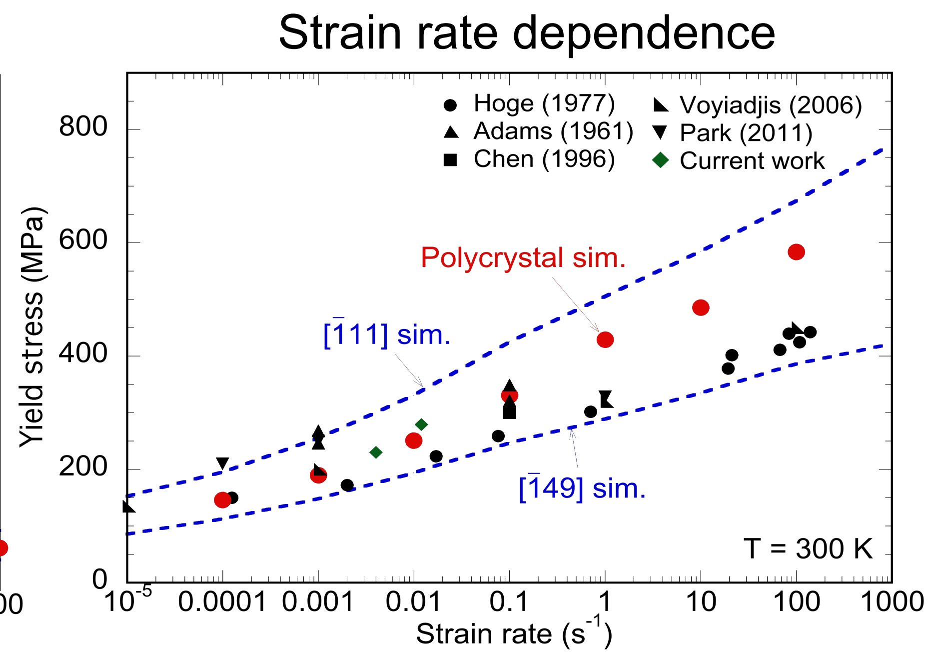

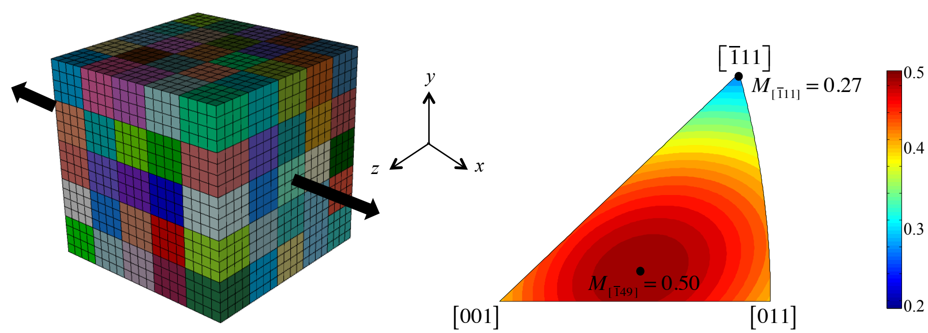

Measured yield stresses of BCC polycrystals lie between the bounds predicted by CP-FEM models on extreme single crystal orientation.

Continuum-Scale Polycrystal Models

- Johnson and Cook (JC) model (Johnson and Cook, 1983, 1985) $\sigma_y^{JC} = A\left(1 + C\ln\dot{\varepsilon}\right)\left(1 - T^{*m}\right)$
- Zerilli-Armstrong (ZA) model (Zerilli and Armstrong, 1987) $\sigma_y^{ZA} = C_0 + C_1\exp\left(-C_3 T + C_4 T\ln\dot{\varepsilon}\right)$
- Mechanical Threshold Stress (MTS) model (Follansbee, 1988) $\sigma_y^{MTS} = \sigma_0 + \hat{\sigma}\left(1 - \left(\frac{k_B T}{G_0}\ln\frac{\dot{\varepsilon}}{\dot{\varepsilon}_0}\right)^{1/q}\right)^{1/p}$

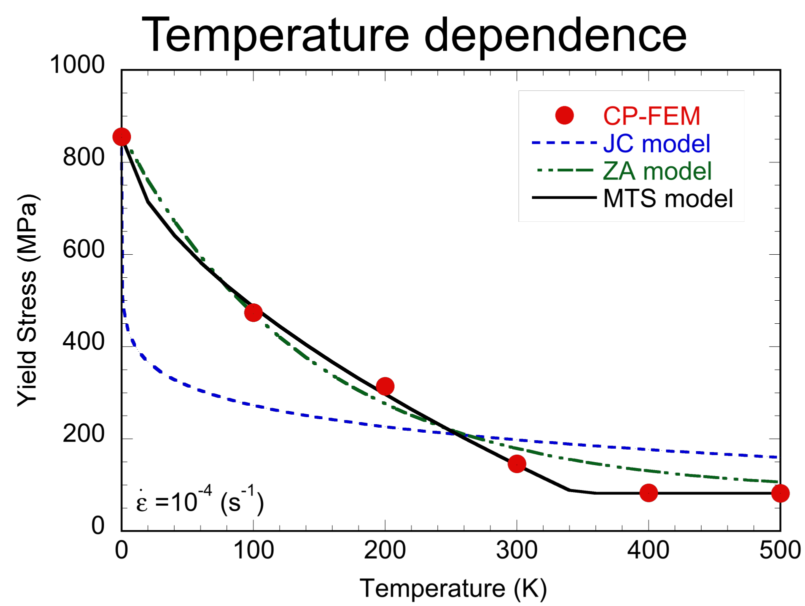

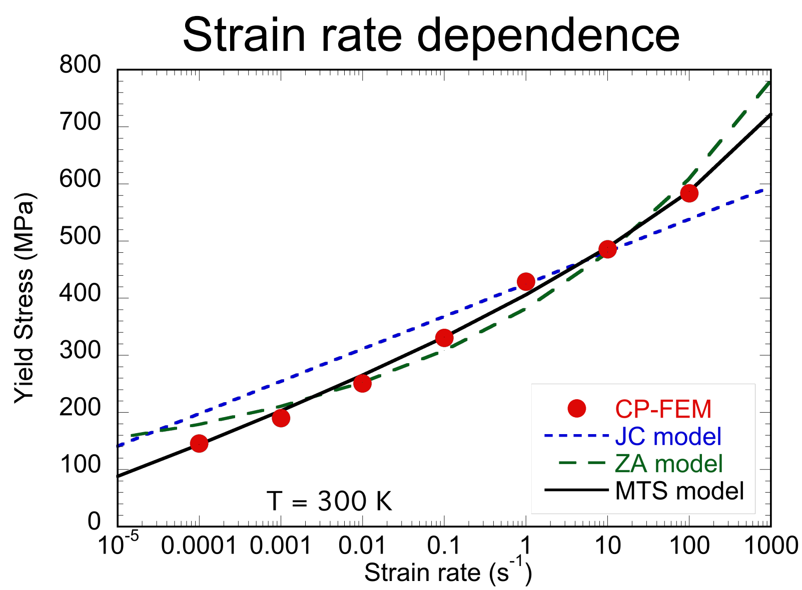

MTS model most accurately reproduces temperature & rate dependent polycrystalline behavior

Hydrodynamics Simulations: Taylor Impact Test

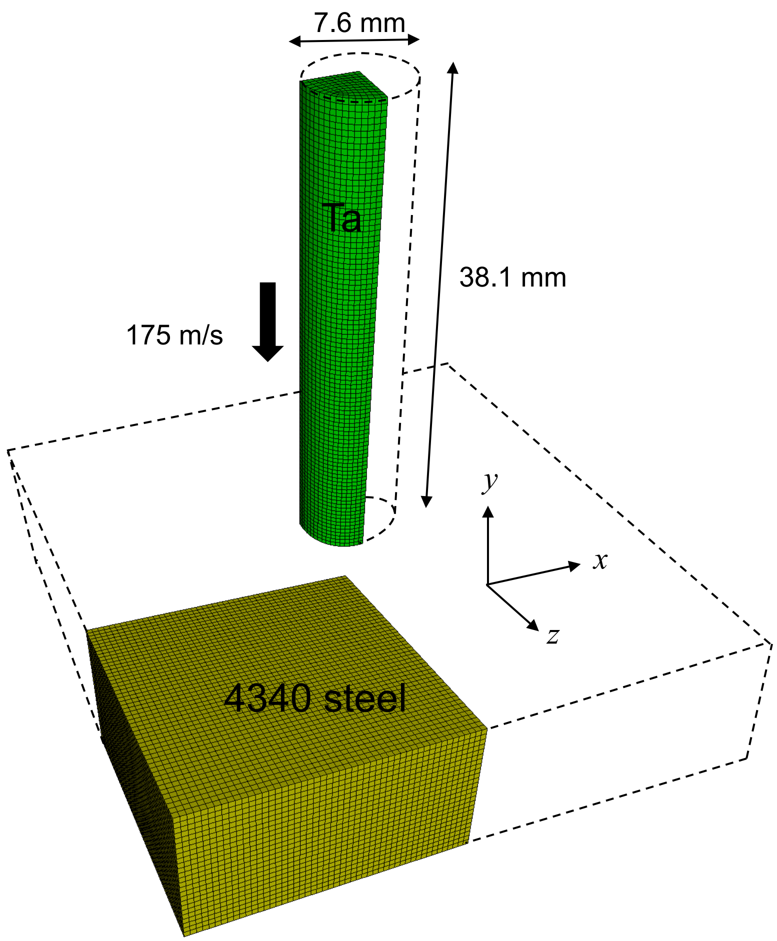

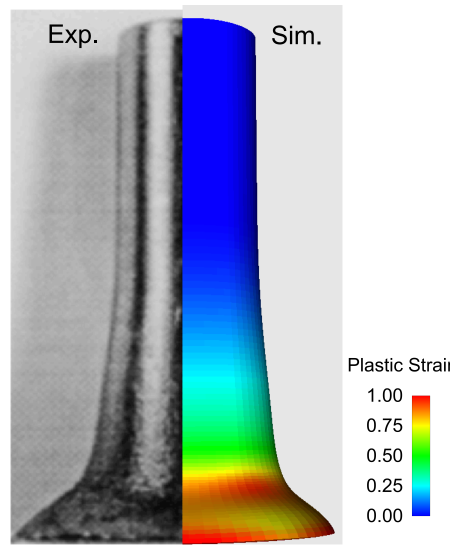

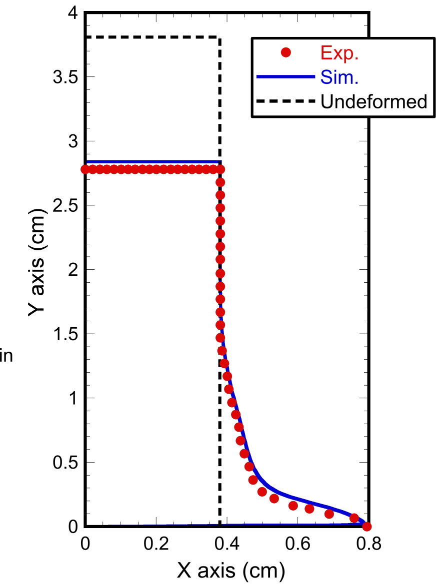

- ALEGRA solid dynamics code (Sandia)
- Kerley Mie-Grüneisen EOS

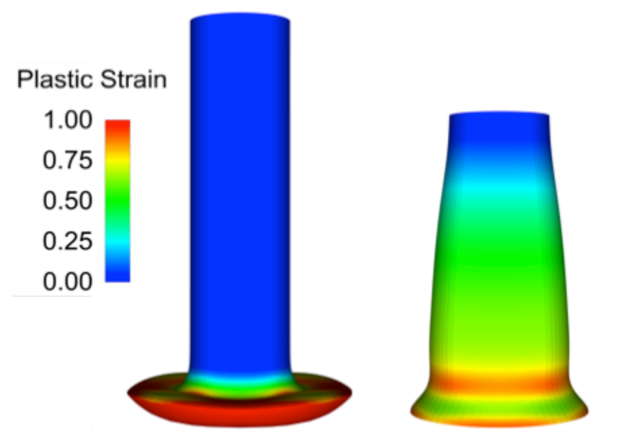

JC model ZA model

* Maudline et al., IJP (1999)

Experimental Validation of CP-FE Simulations of Ta Oligocrystals

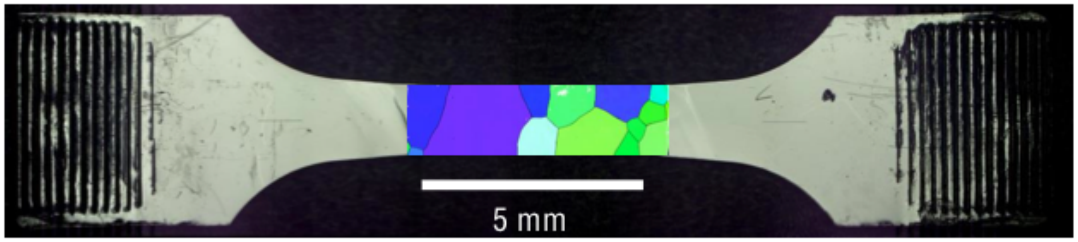

- Lim, H., Carroll, J. D., Battaile, C. C., Weinberger, C. R., Boyce, B. L., 2015. "Quantitative Comparison between Experimental Measurements and CP-FEM Predictions of Plastic Deformation in a Tantalum Oligocrystal", Int. J. Mech. Sci., 92, 98–108.
- Lim, H., Carroll, J. D., Battaile, C. C., Buchheit, T. E., Boyce, B. L., Weinberger, C. R., 2014. "Grain- scale Experimental Validation of Crystal Plasticity Finite Element Simulations of Tantalum Oligocrystals" Int. J. Plasticity, 60, 1–18.

Experimental Setup

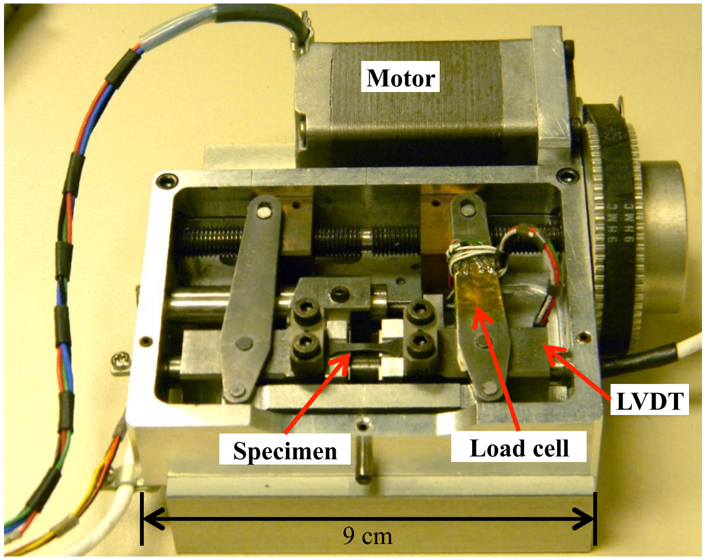

- Tantalum oligocrystals with mostly columnar 2D grain structure eliminate unknown subsurface grain morphology.
- *In-situ* load frame developed at Sandia
- HR-DIC (surface strain fields) and EBSD (crystal orientations) measurements at load inside SEM

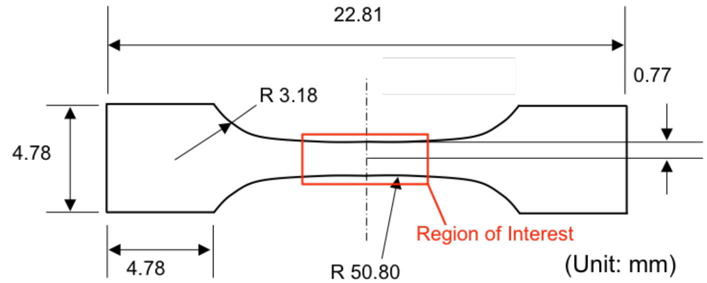

Specimen 1

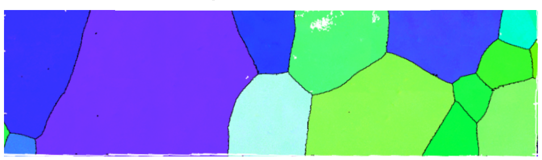

Specimen 2

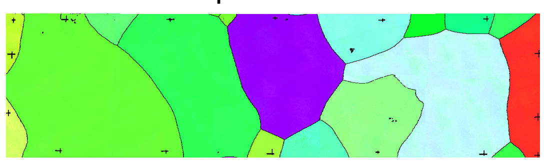

Specimen 3

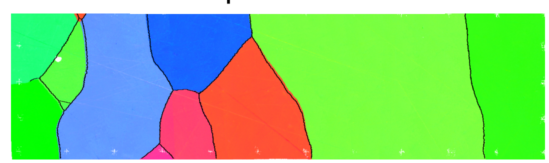

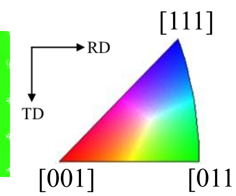

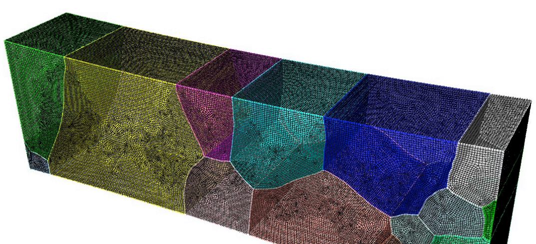

15 grains
(1,426,650 elements)

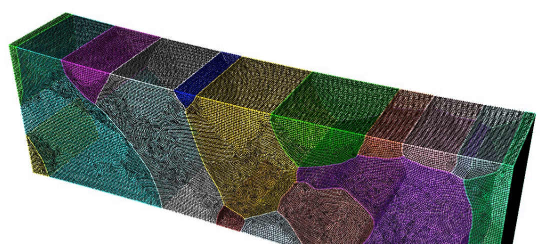

18 grains
(1,664,150 elements)

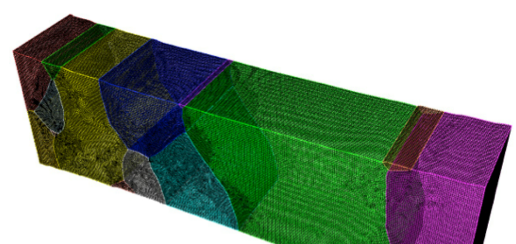

12 grains
(2,140,020 elements)

Strain Field Analysis

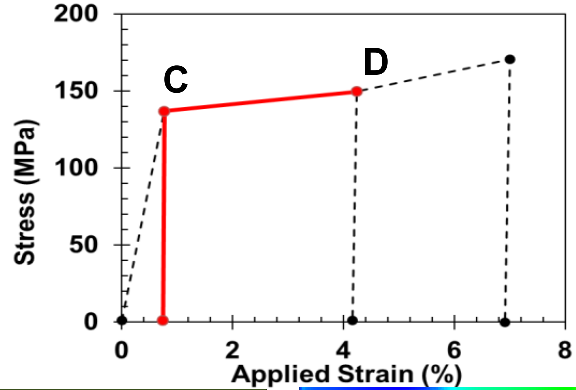

$\Delta\varepsilon_{CD}$ =3.4%

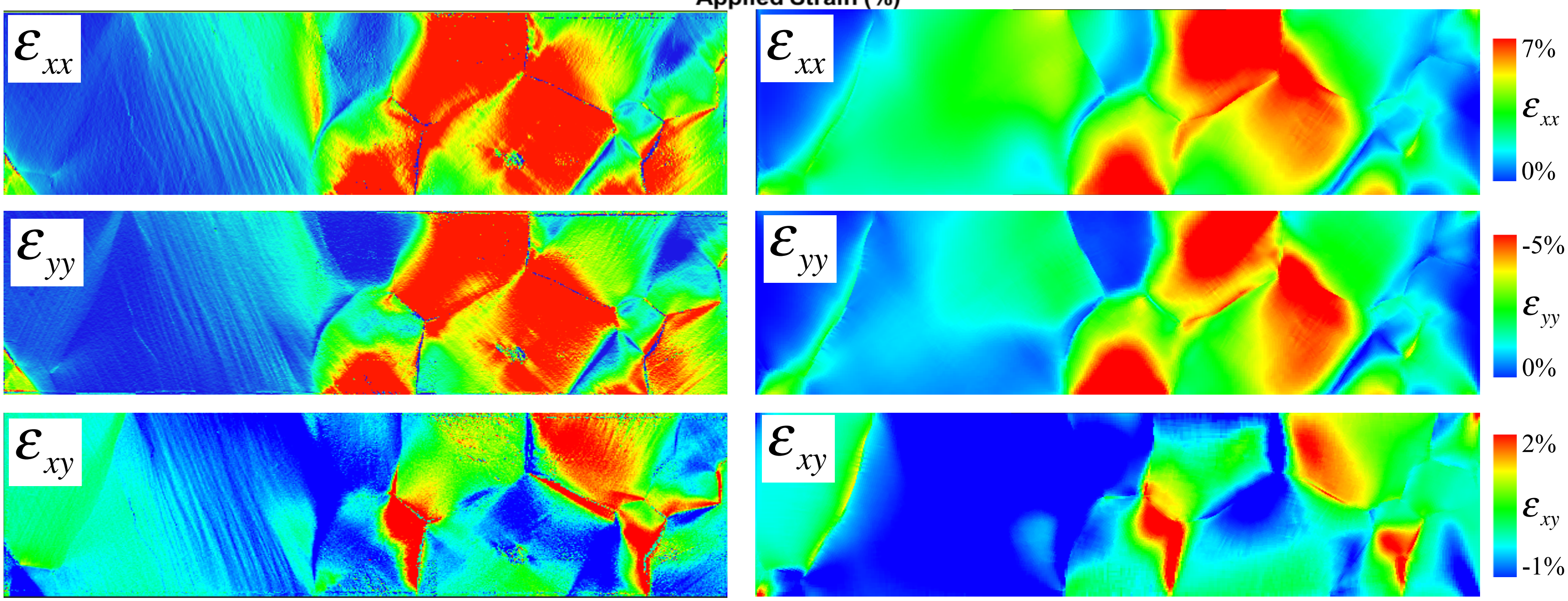

(a) HR-DIC measurements (b) CP-FEM predictions

Measured and predicted strain fields agree well quantitatively.

Out-of-plane Displacement Gradients

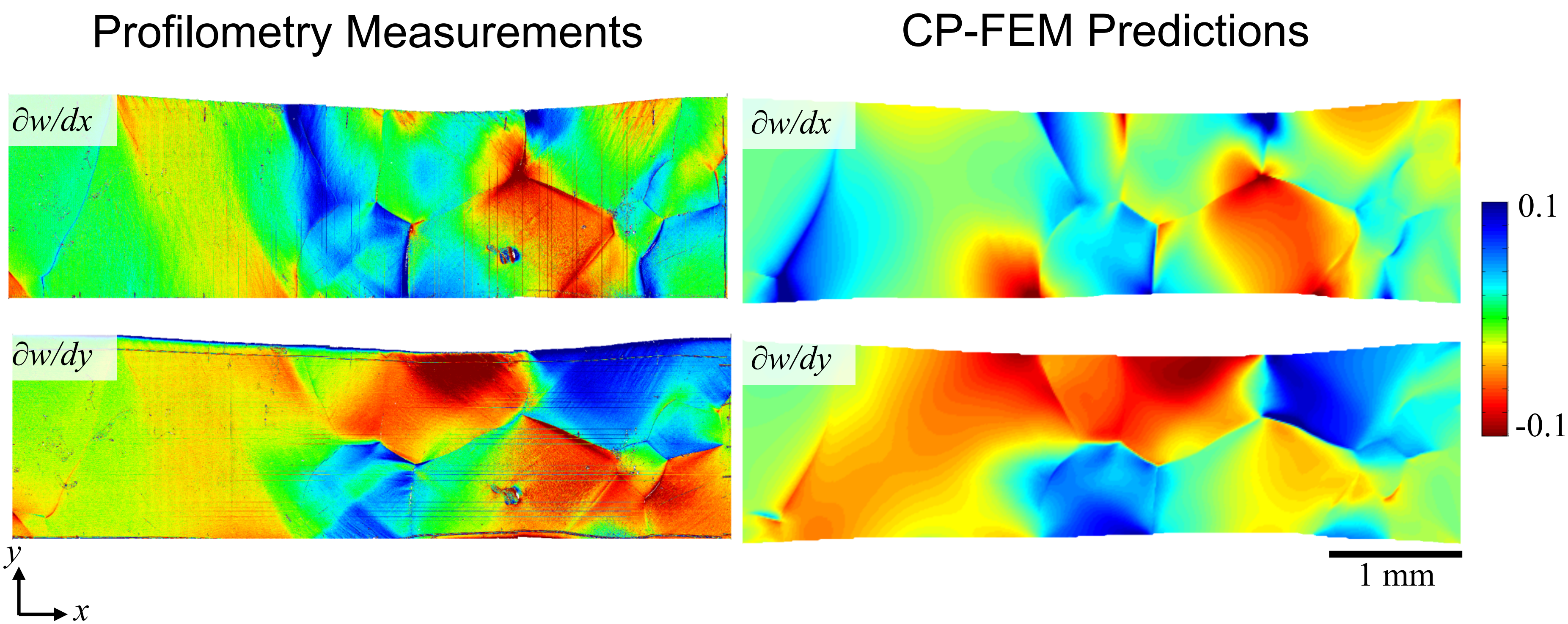

Measured and predicted out-of-plane displacement fields agree reasonably well.

Specimen 1
Applied strain = 6.8%

CP-FEM Predictions of Crystal Rotation

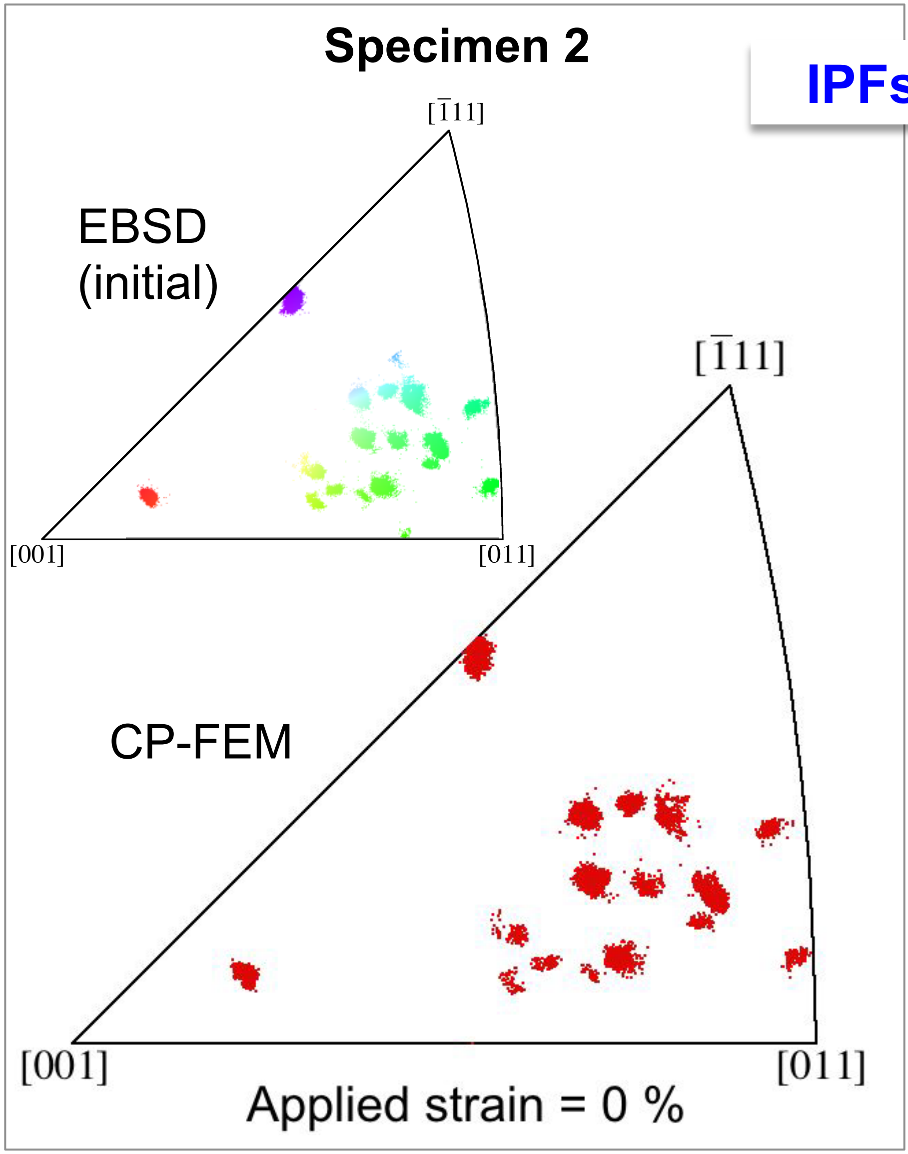

IPFs in RD

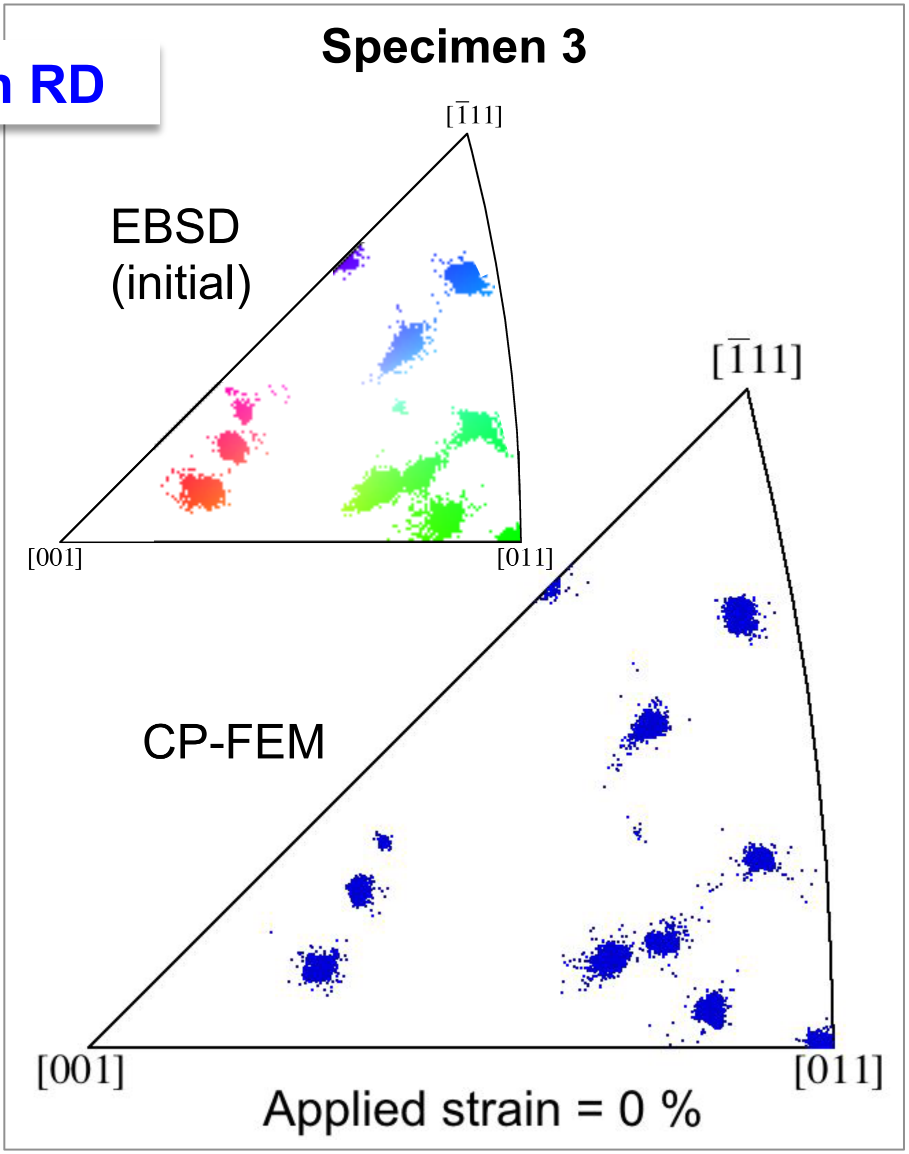

Texture Predictions

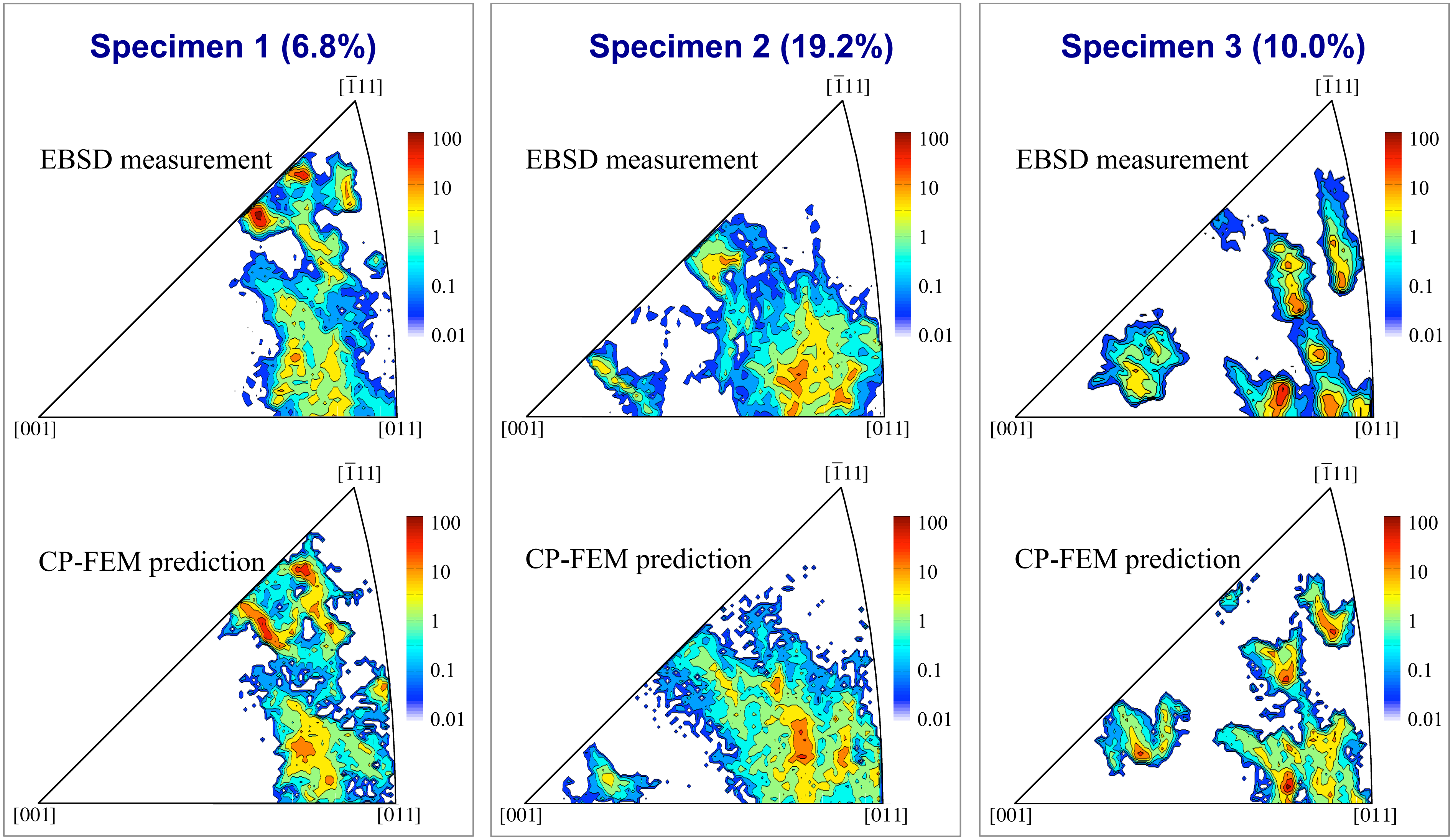

IPF contour plots indicate very good agreement between model and experiment.

Failure Analysis

Ta oligocrystal specimen 2 at 19.2% deformation

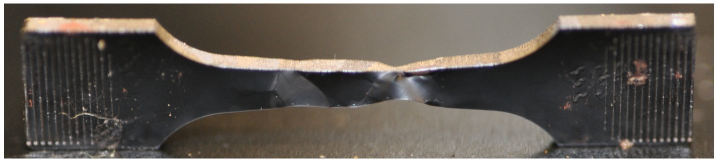

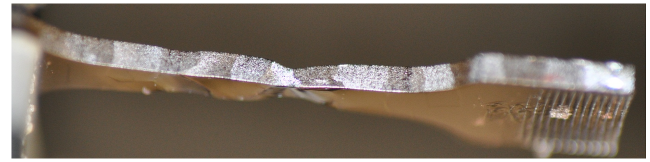

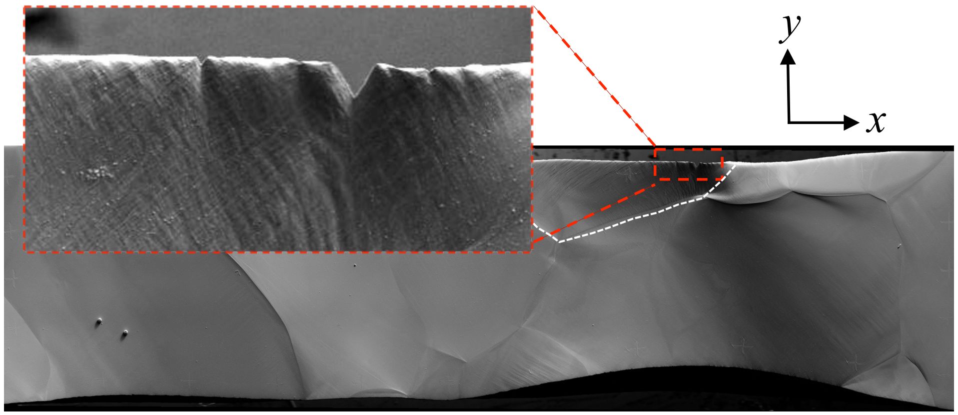

Surface image (side view)

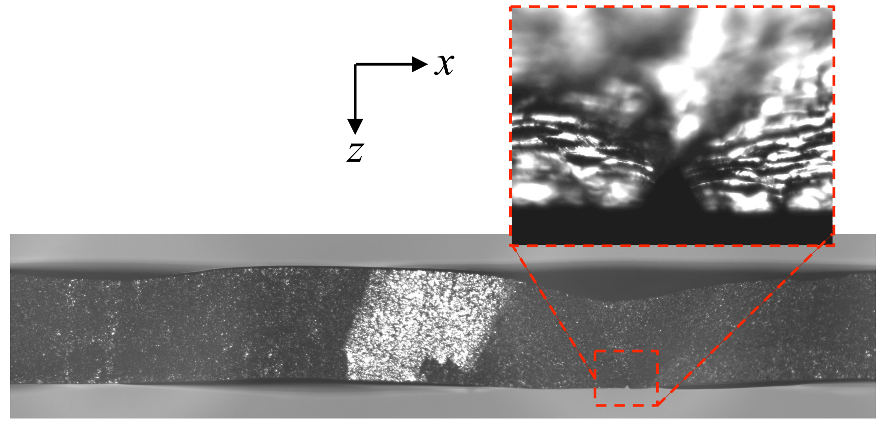

Surface image (top view)

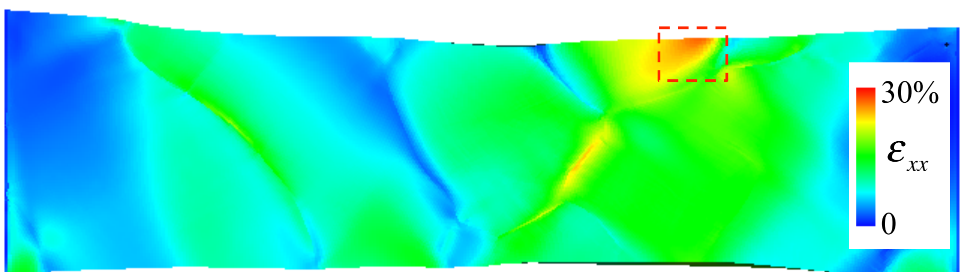

Simulated ε_{xx} (side view)

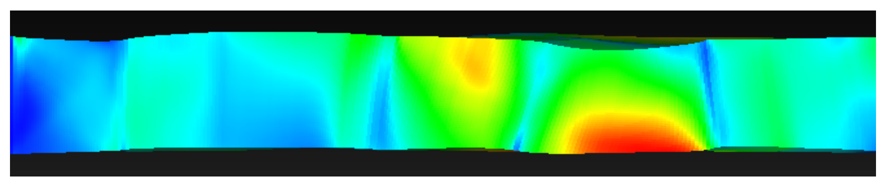

Simulated ε_{xx} (top view)

Failure location agrees with location of the highest ε_{xx} from the simulation

Grain-scale Microstructural Variability

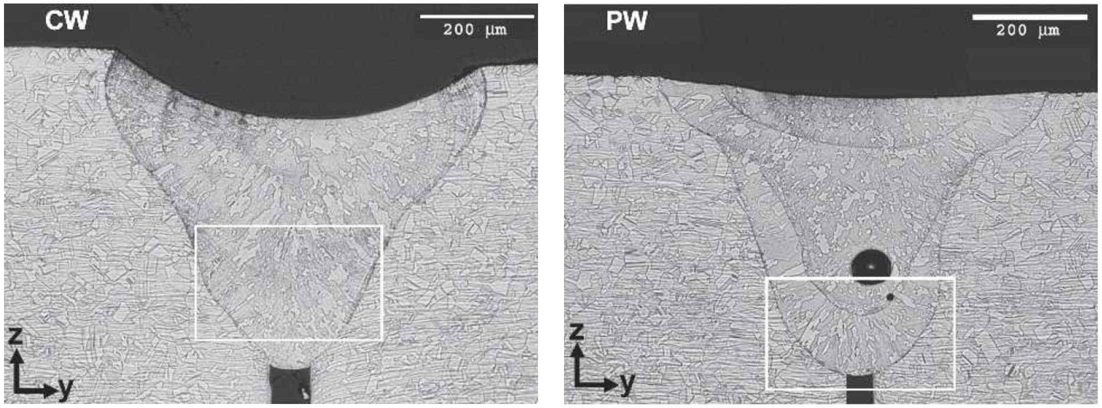

Microstructural details vary
among 304L stainless steel weldments

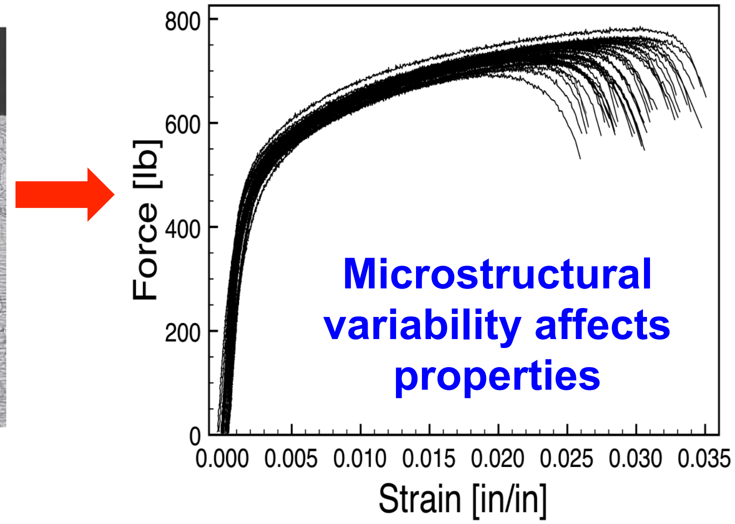

Simulation of Ta Notch

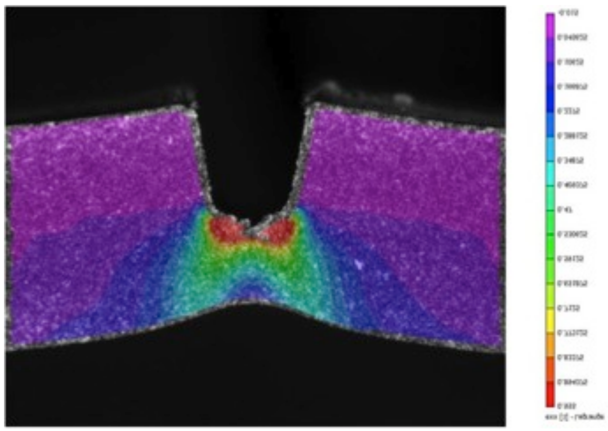

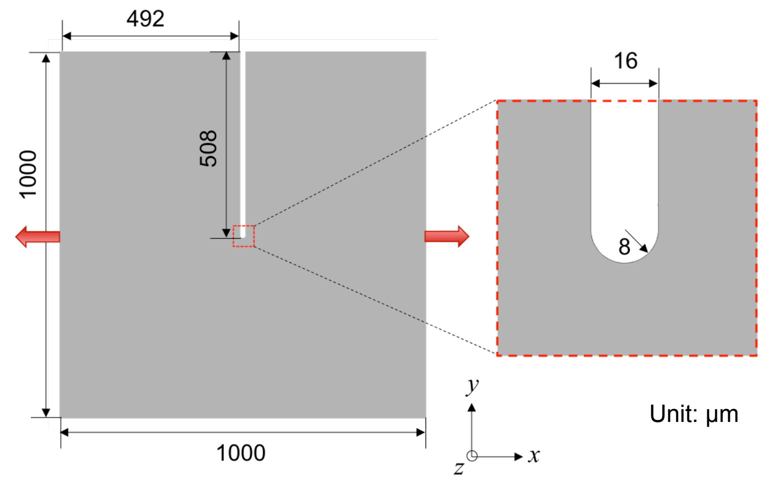

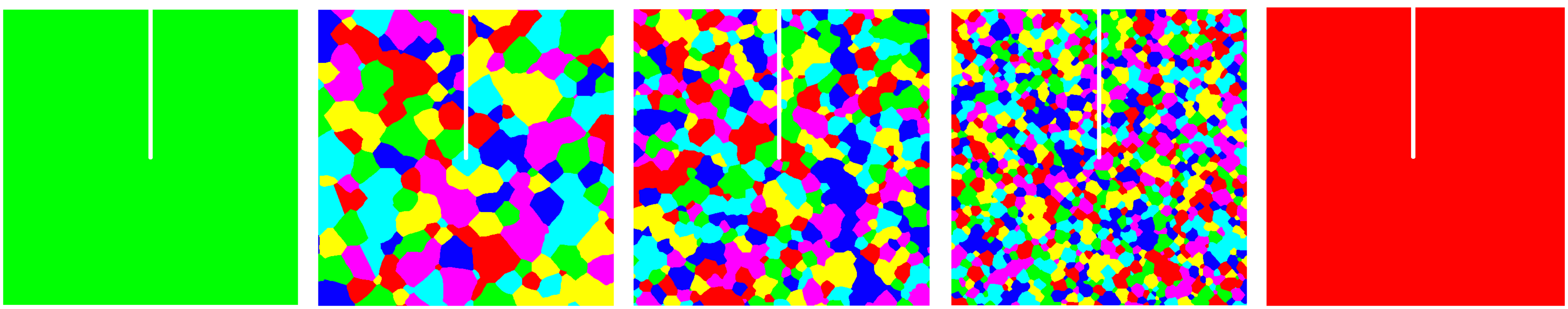

CP-FEM: 1 grain (111696 elements) Grain size > 1 mm

CP-FEM: 204 grains (115579 elements) Grain size = 70 µm

CP-FEM: 482 grains (111696 elements) Grain size = 45 µm

CP-FEM: 1184 grains (83,657 elements) Grain size = 30 µm

J2 FEM model (83,386 elements)

d: grain diameter *l*: notch length

100 CP-FEM simulations with random texture (i.e. 100 microstructural realizations)

Deformation of Ta Notched Specimen

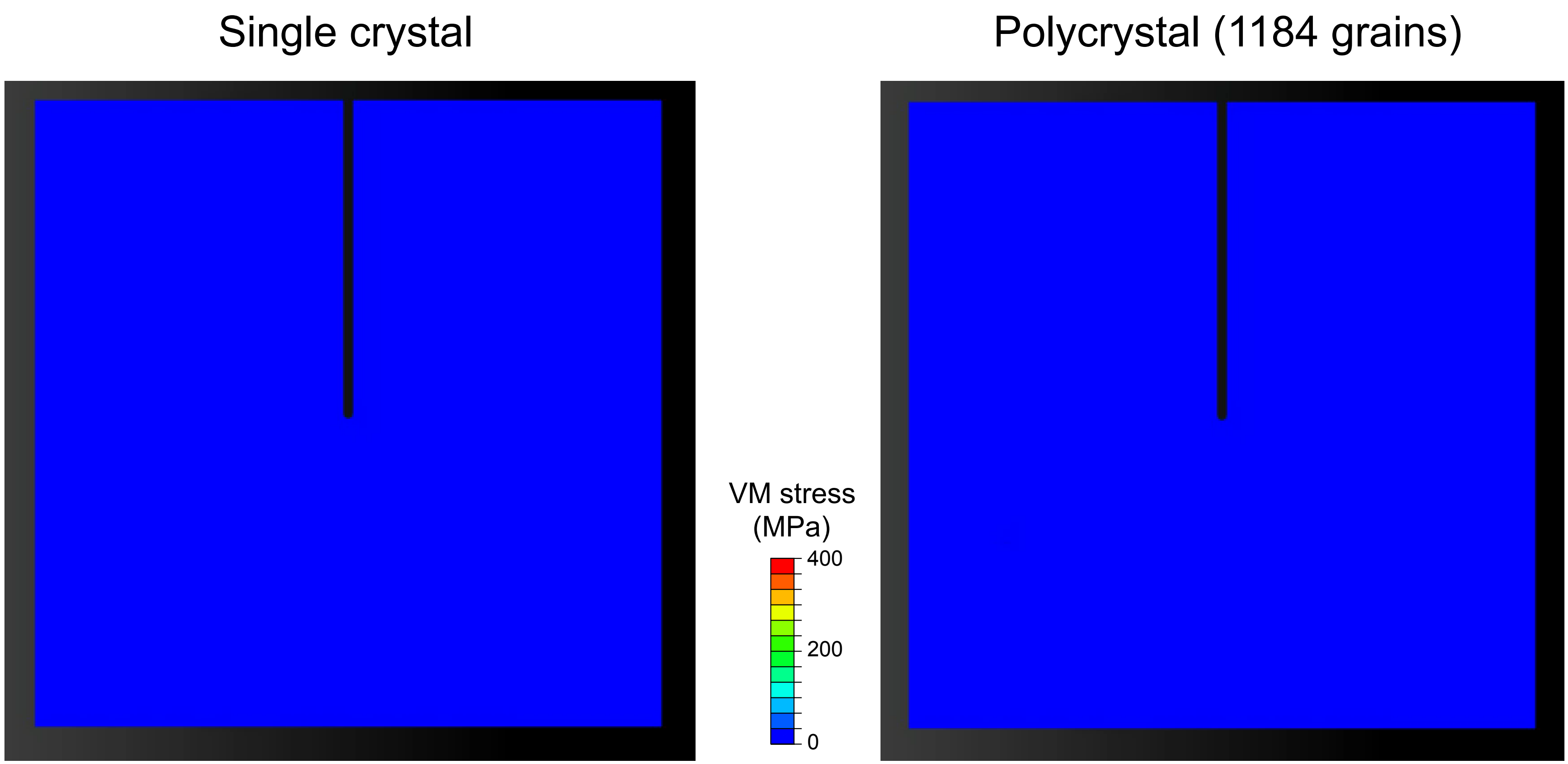

Simulations of Notched Ta

Connecting microstructural variability to stochastic performance

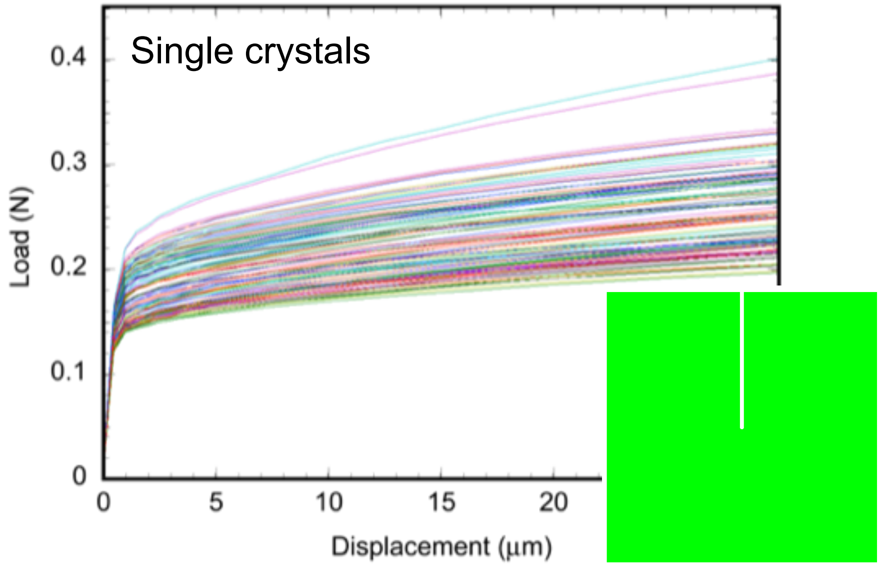

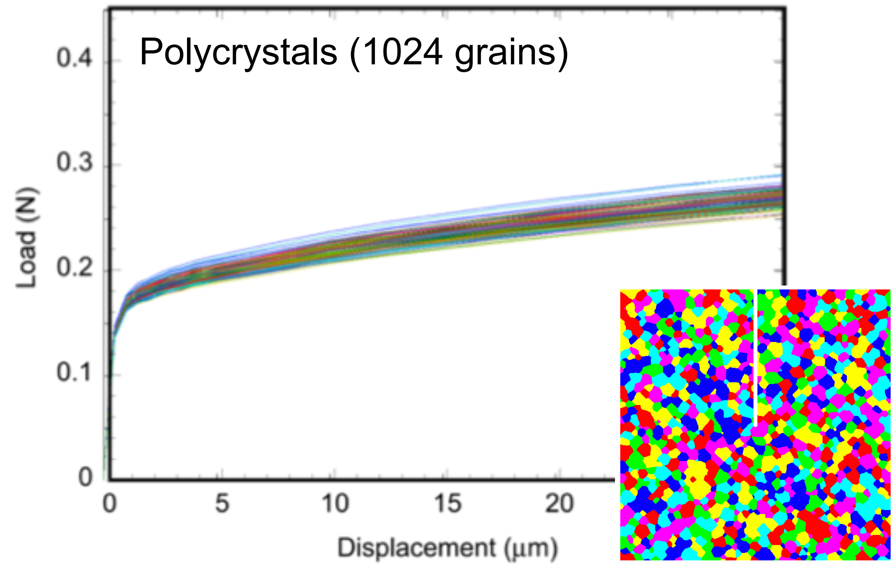

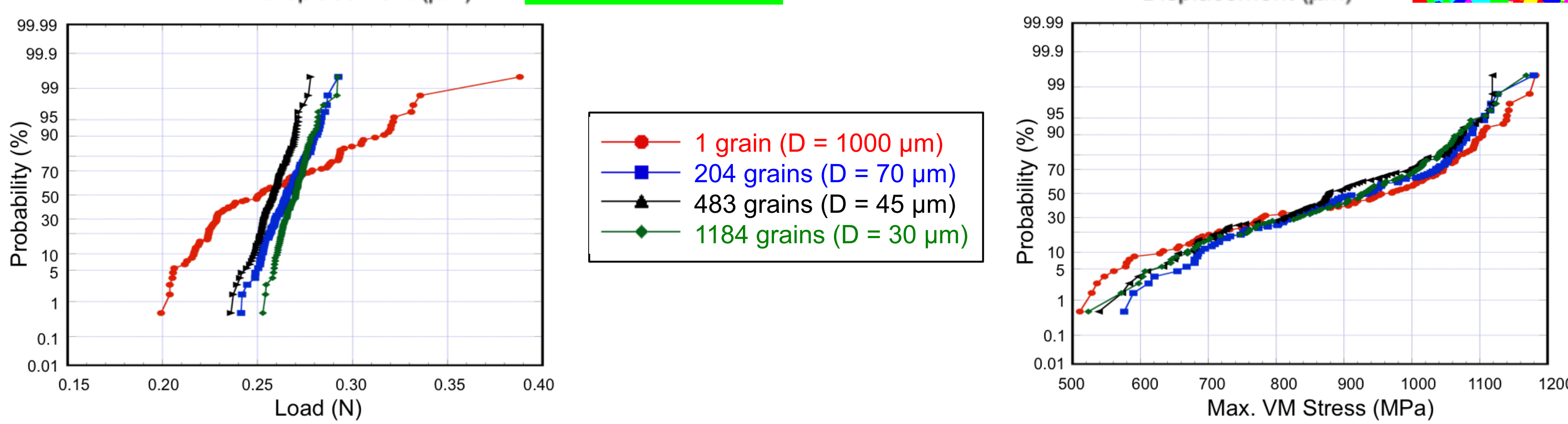

Variability in load-displacement and localized max VM stress from 100 realizations.

Experiment - Simulation Comparisons

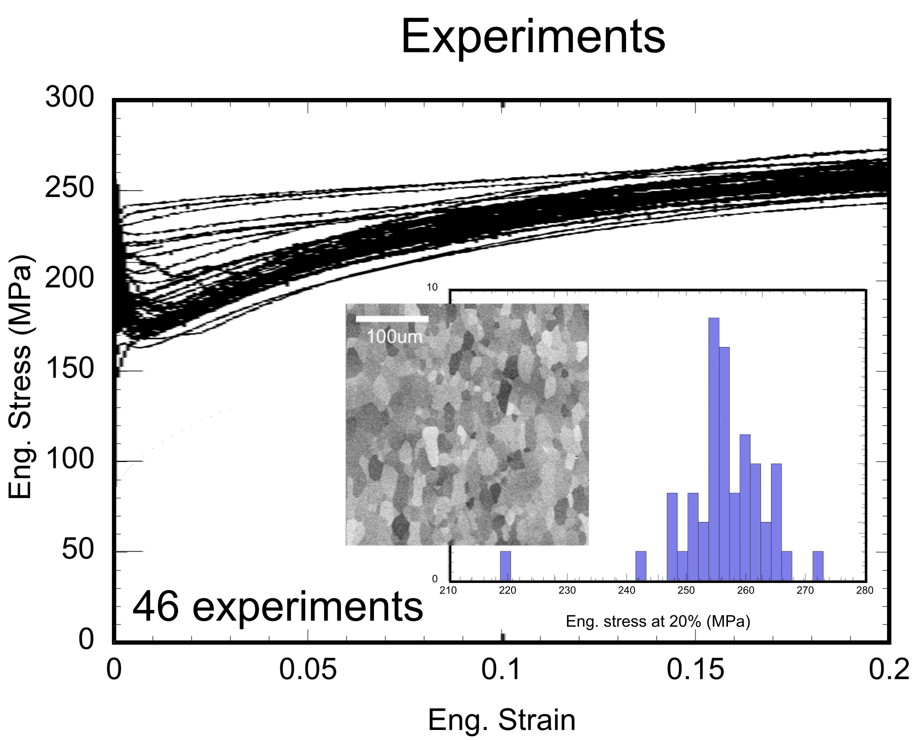

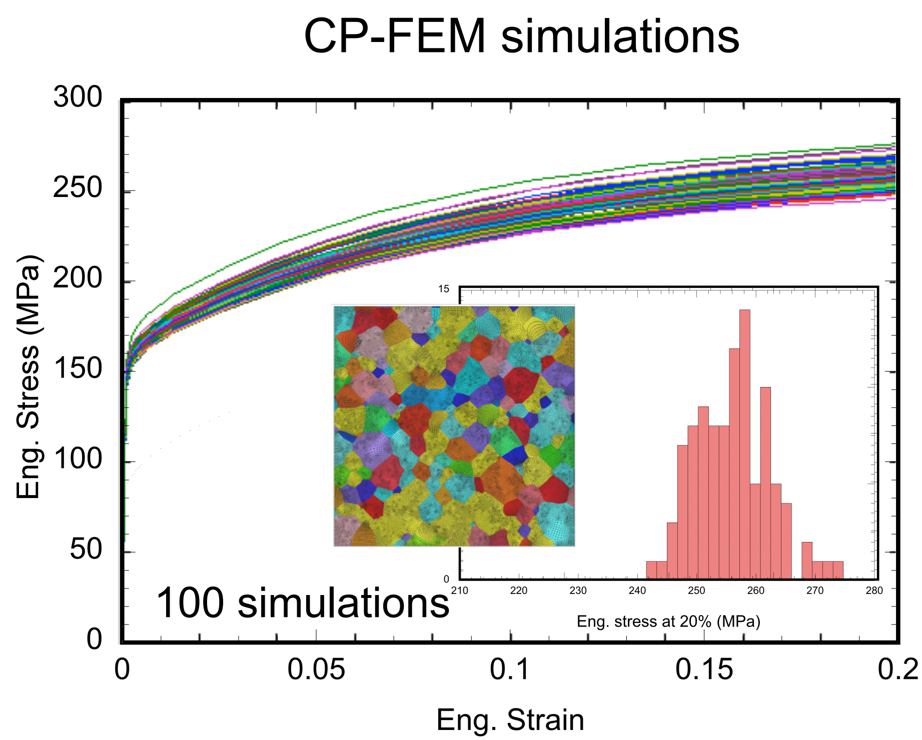

CP-FEM model captures grain-scale variability in mechanical responses of polycrystalline tantalum

Microstructure Modeling using Phase Field Grain Growth Model

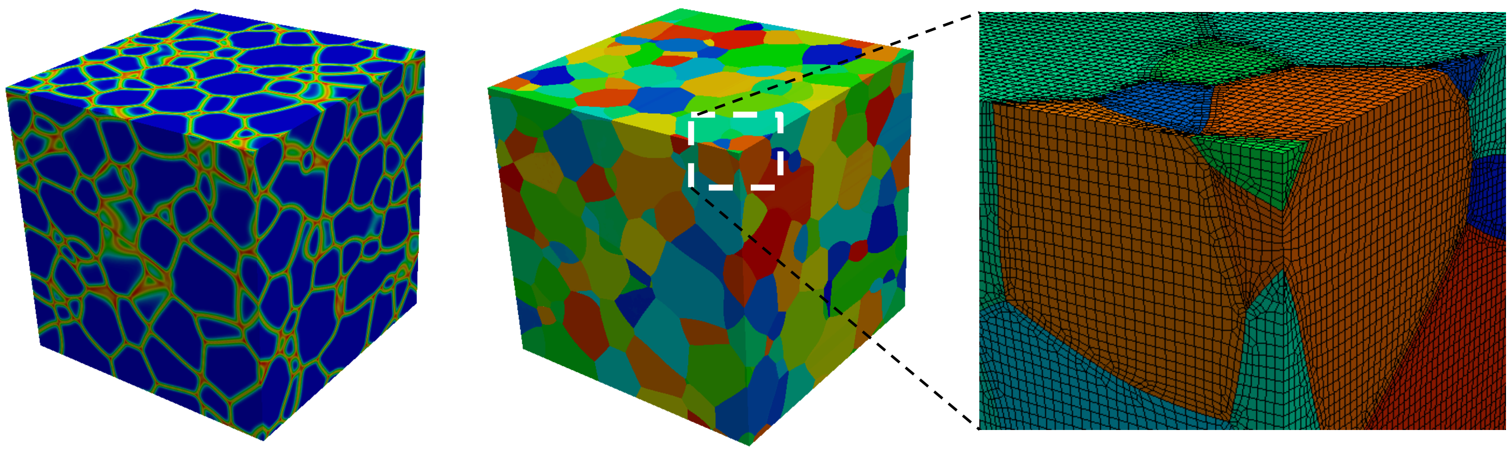

Motivation

Large-scale continuum simulations with microstructure fidelity are hindered by limited capabilities to model realistic 3D microstructures (Fig (a)).

- Most finite element based polycrystalline models use idealized grain shapes or Voronoi tesselations (Fig. (b)).
- 3D microstructures digitized from experiments conform to a uniform grid. (Fig. (c))

(a)

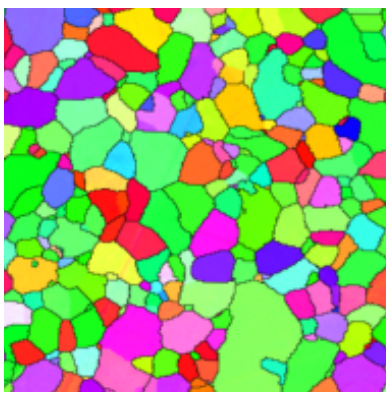

(b)

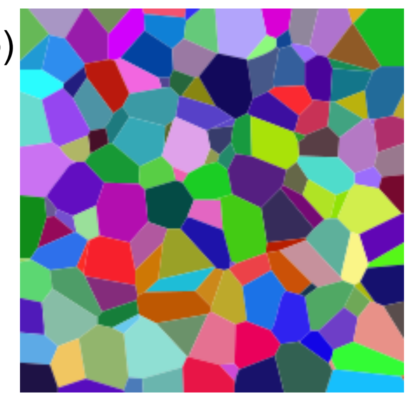

(c)

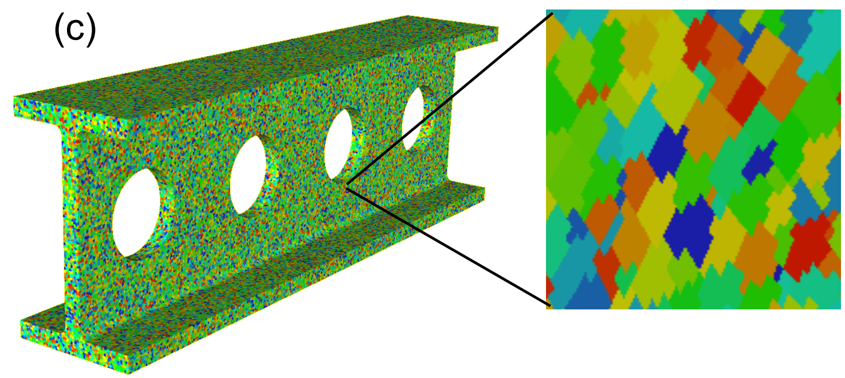

Microstructures from (a) electron back scatter diffraction, (b) Voronoi tesselation and (c) voxelated 3D structure of I-beam [Bishop et al., 2014].

Need a technique to create physically-based three-dimensional microstructures!

Approach: Phase Field to CP-FEM

Sandia National Laboratories

PHASE FIELD GRAIN GROWTH SIMULATIONS → **CRYSTAL PLASTICITY FINITE ELEMENT SIMULATIONS**

CUBIT 'SCULPT' TECHNOLOGY

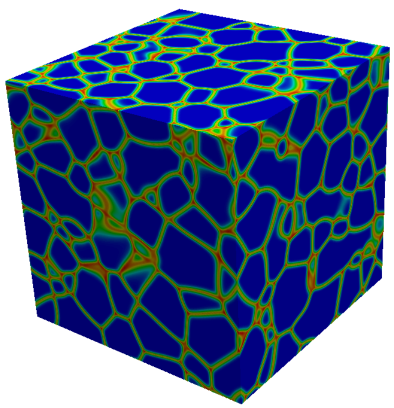

Realistic 3D microstructure
Conformal grain boundary mesh
Generates hexahedral elements

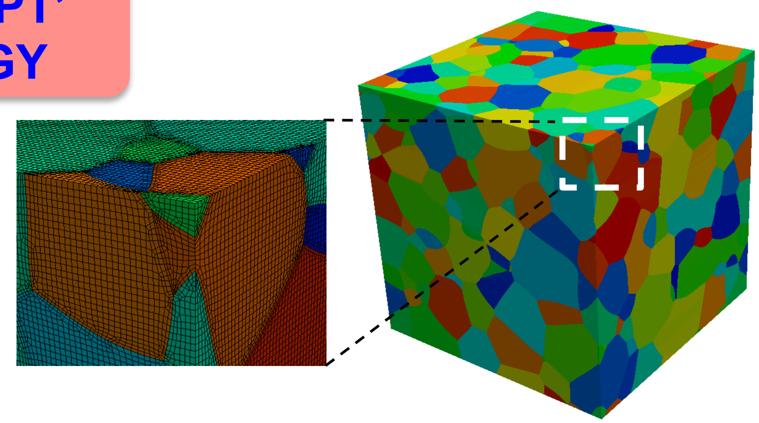

SCULPT interface reconstruction

$v_A = 0.73$ $v_B = 0.27$	$v_A = 0.41$ $v_B = 0.59$	$v_A = 0.43$ $v_B = 0.57$
$v_A = 0.00$ $v_B = 1.00$	$v_A = 0.55$ $v_B = 0.45$	$v_A = 0.38$ $v_B = 0.62$
$v_A = 0.00$ $v_B = 1.00$	$v_A = 0.79$ $v_B = 0.21$	$v_A = 1.00$ $v_B = 0.00$

Volume fractions representing percent of grains for each cell

Resolve grain interfaces and project nodes to surfaces

Insert layer of hex elements at interfaces

Perform smoothing

Spherical Grain within a Cubic Matrix

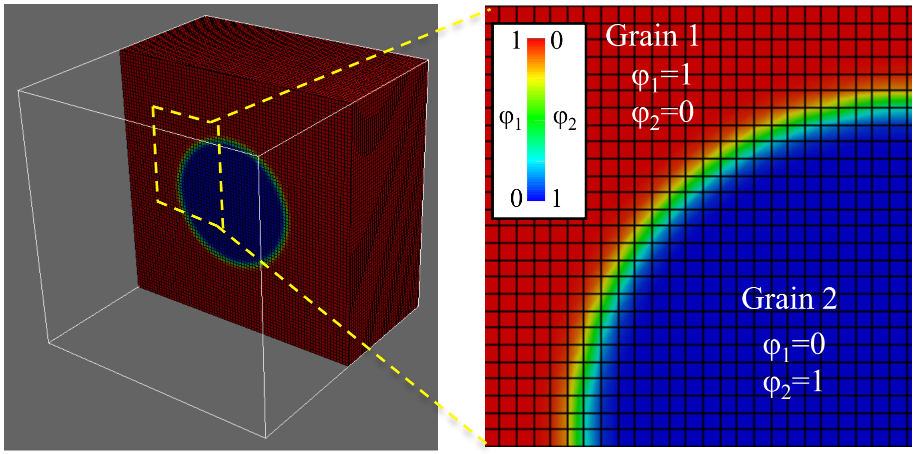

Phase field grain growth

❖Total free energy

$$\mathcal{F}_{tot} = \int d\mathbf{r} \left\{ \frac{4}{3} \left[1 - 4 \sum_{i=1}^{n_\phi} \phi_i^3 + 3 \left(\sum_{i=1}^{n_\phi} \phi_i^2 \right)^2 \right] + \sum_i^{n_\phi} \frac{\epsilon_i^2}{2} |\nabla \phi_i|^2 \right\}$$

❖Dynamics

$$\frac{\partial \phi_i}{\partial t} = -L_i \left(\frac{\delta \mathcal{F}_{tot}}{\delta \phi_i} \right)$$

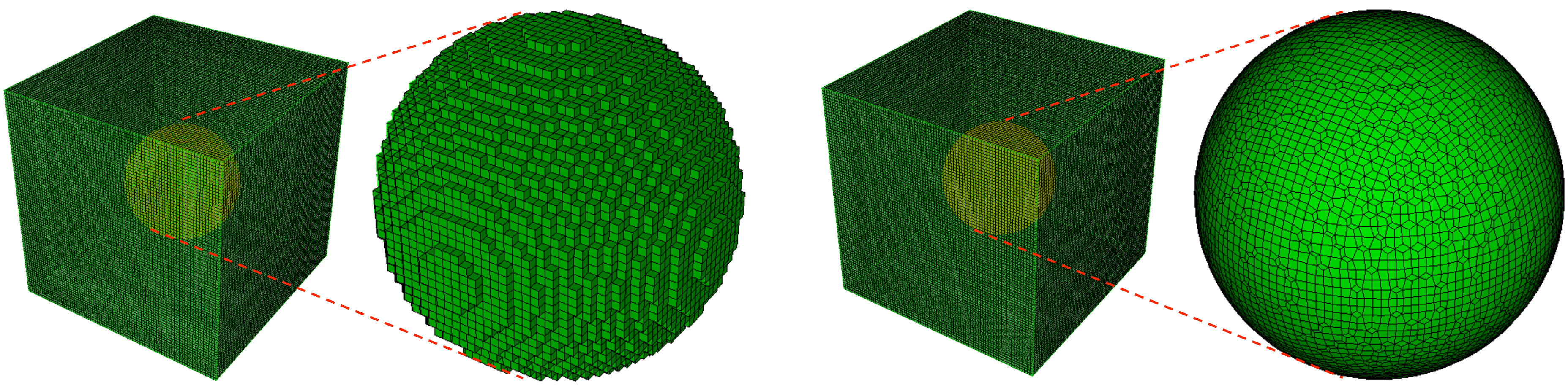

FE mesh

Phase Field Grain Growth Results to FE Mesh

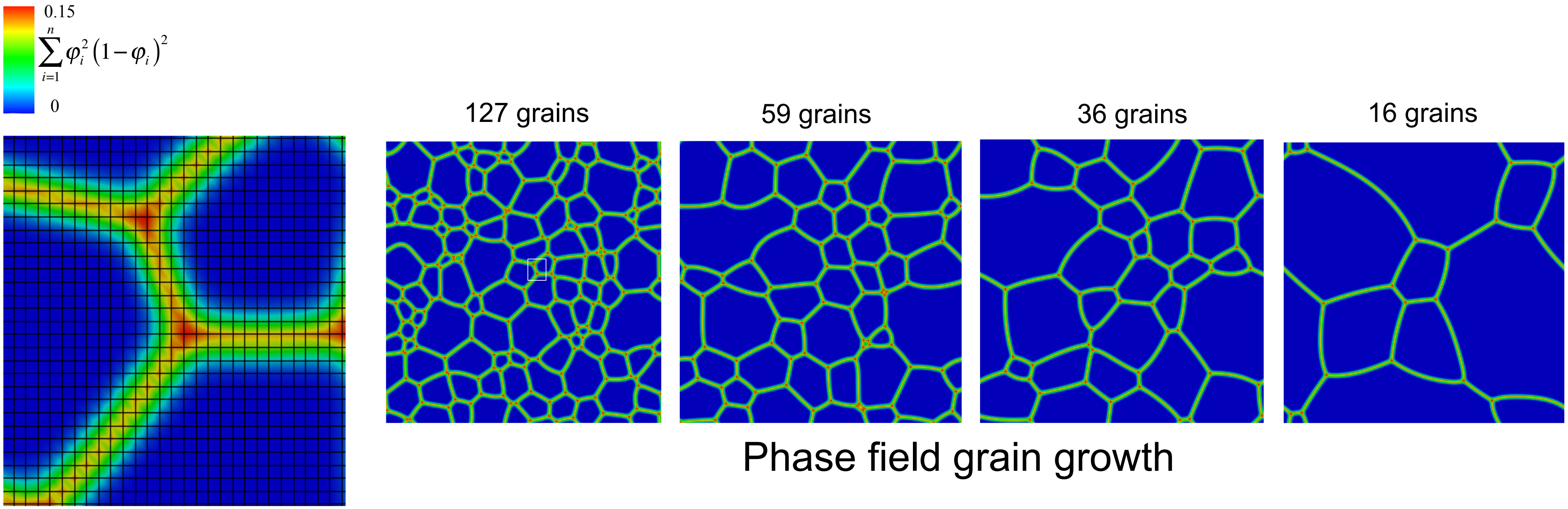

Phase field grain growth

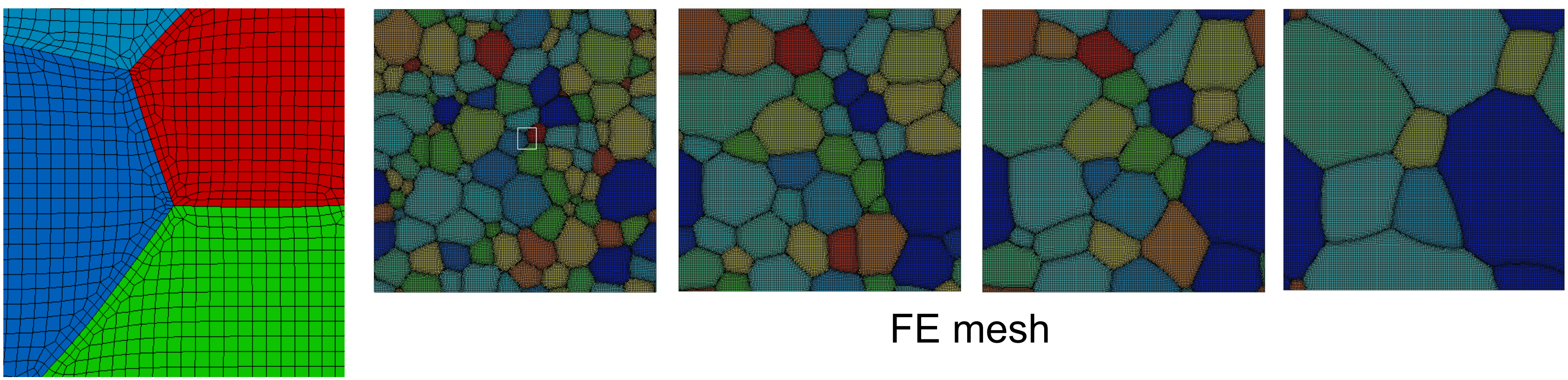

FE mesh

FE mesh of 3D Polycrystalline Microstructure

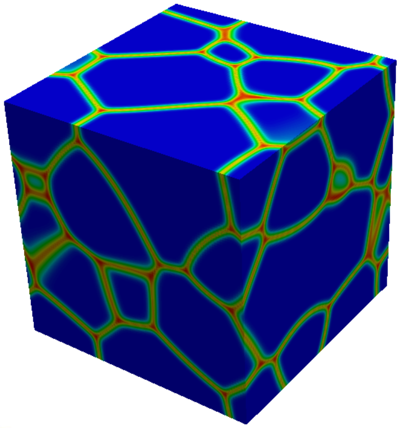

Voxelated FE mesh

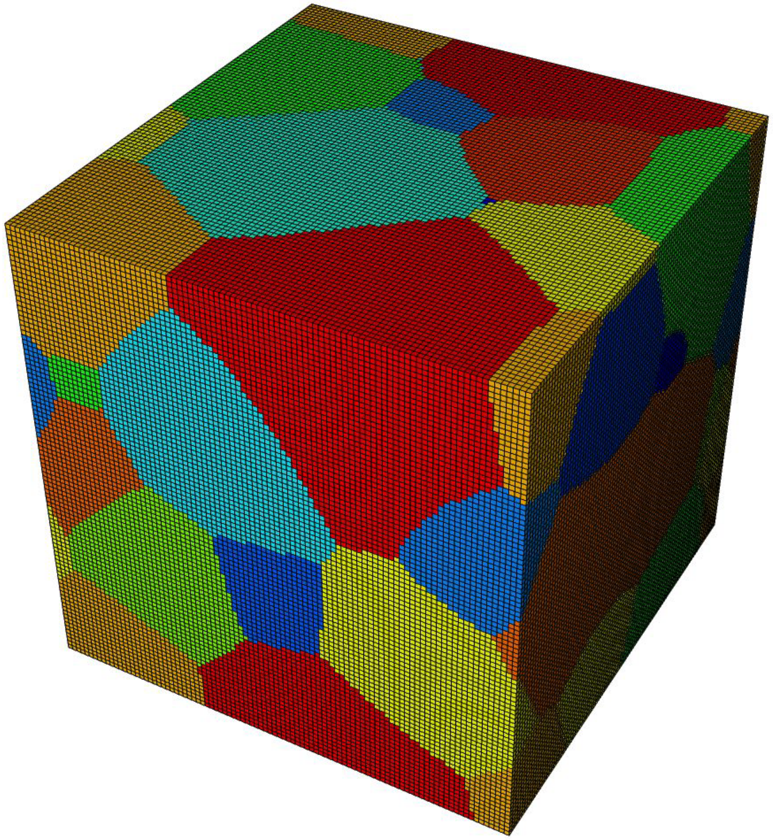

Conformal FE mesh

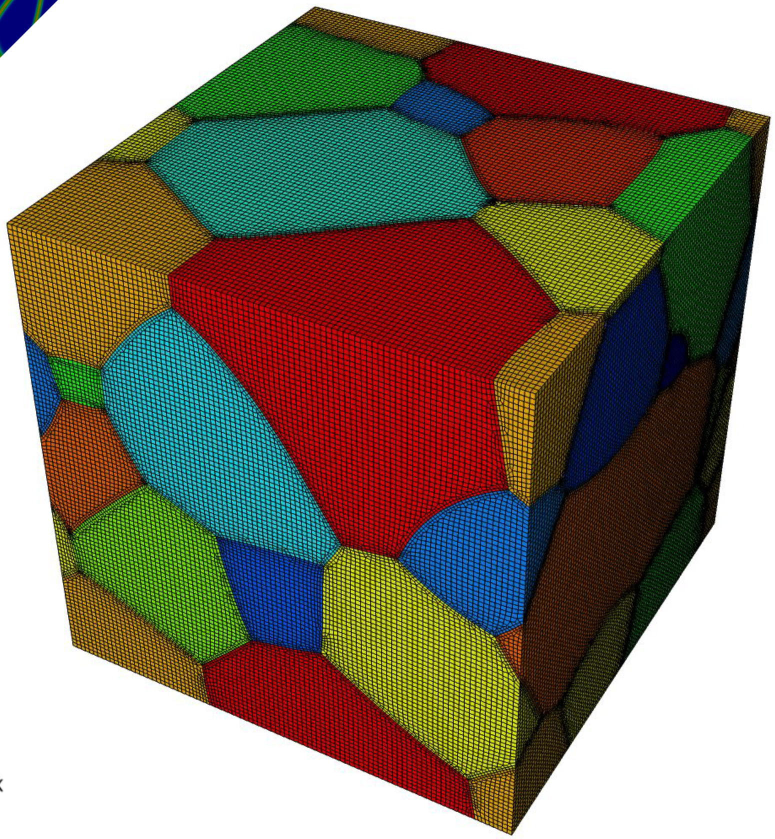

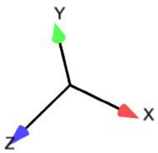

Stress Distributions at 10% Deformation

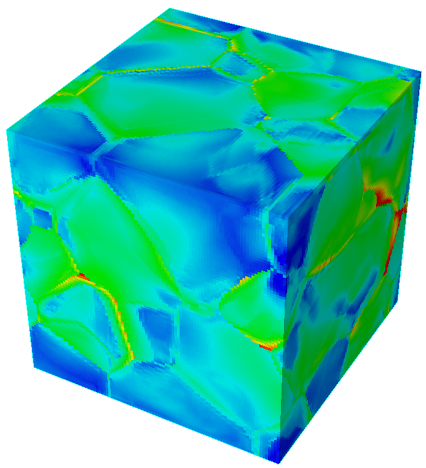

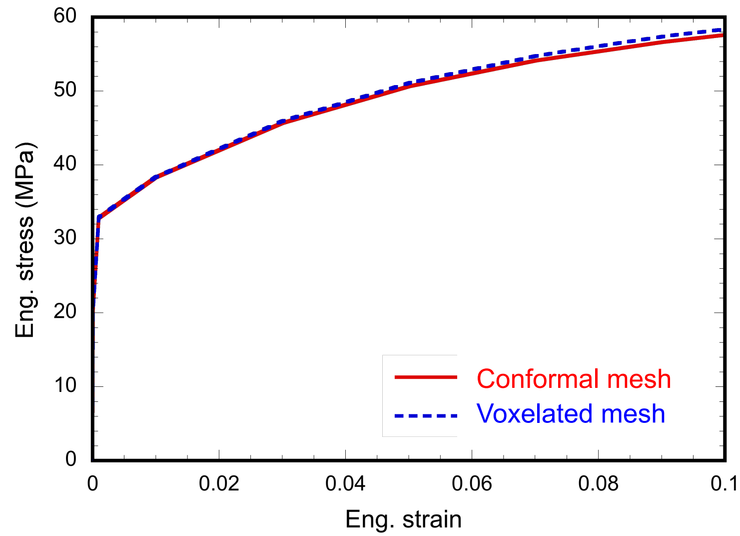

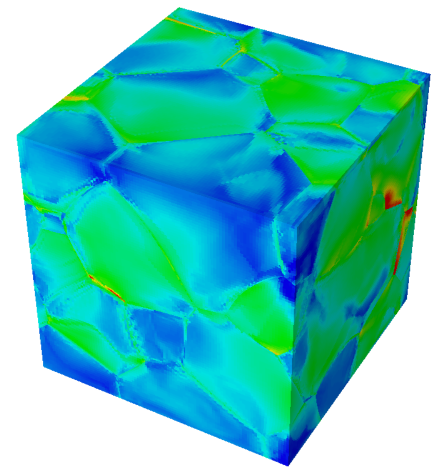

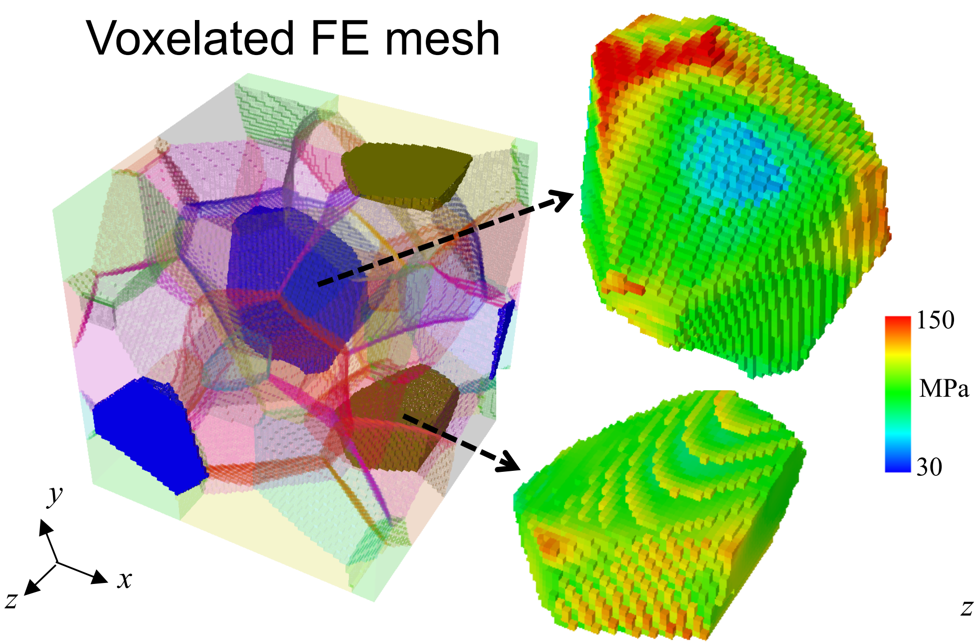

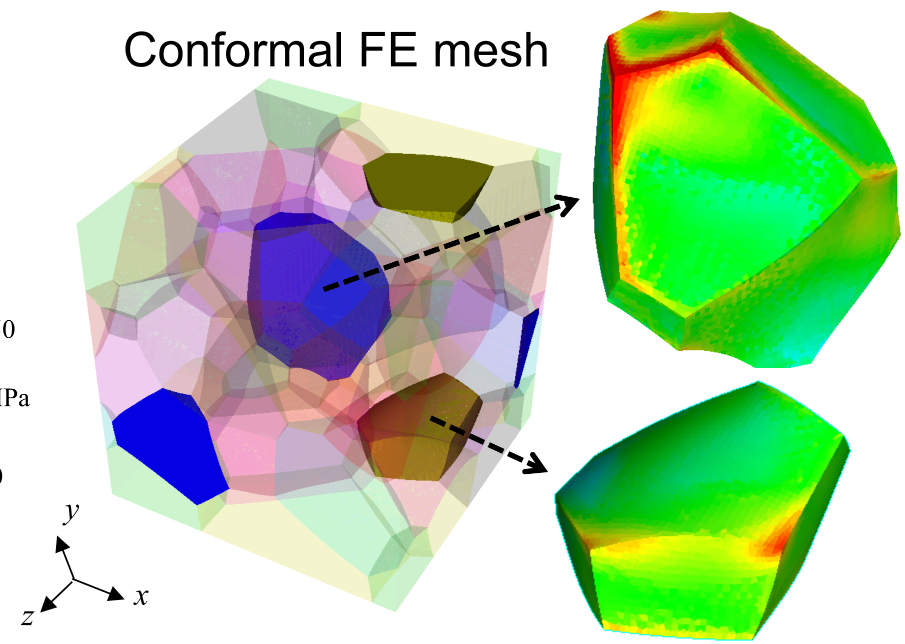

Mesh Sensitivity Tests

Voxelated FE mesh

Conformal FE mesh

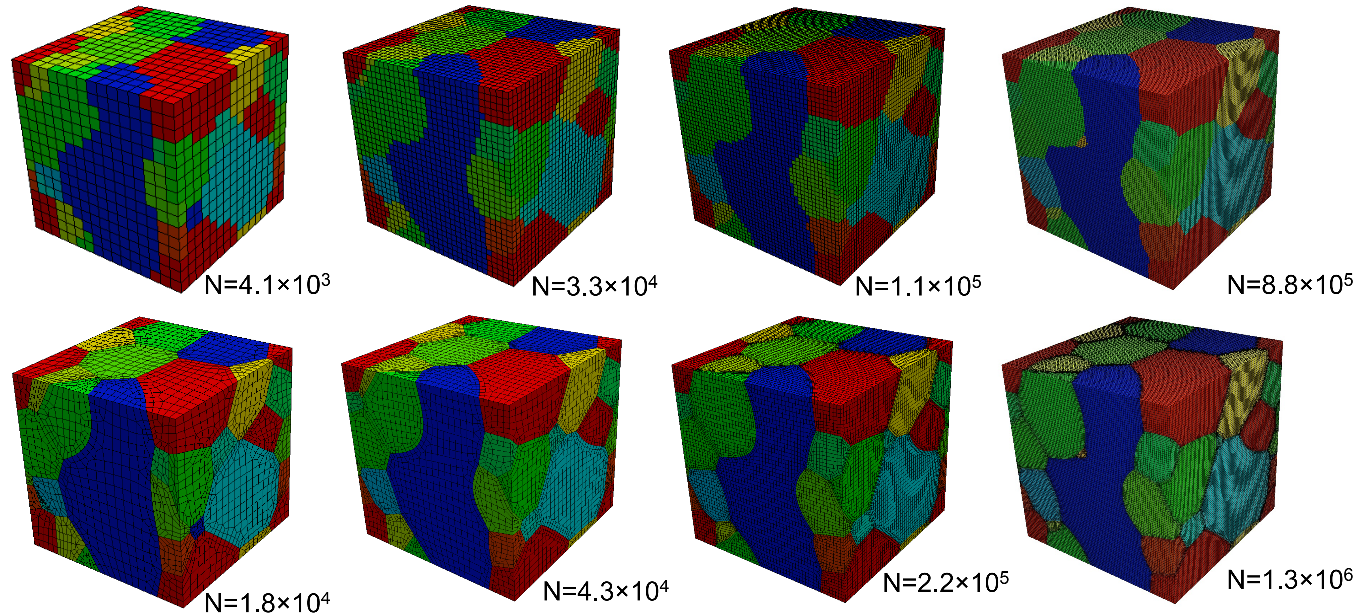

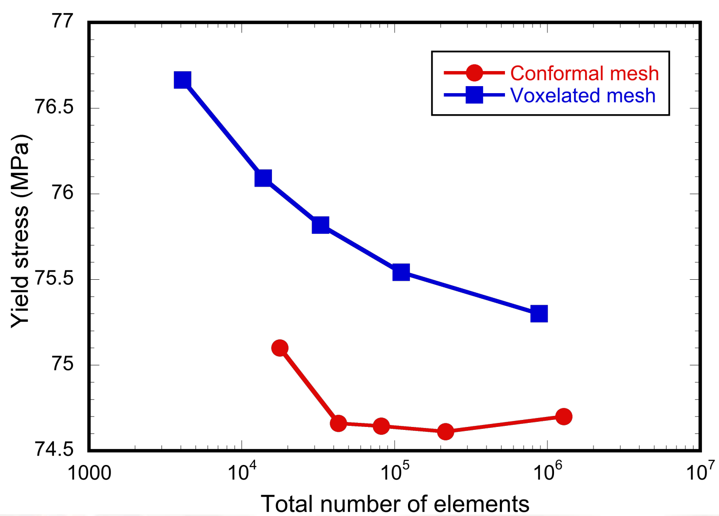

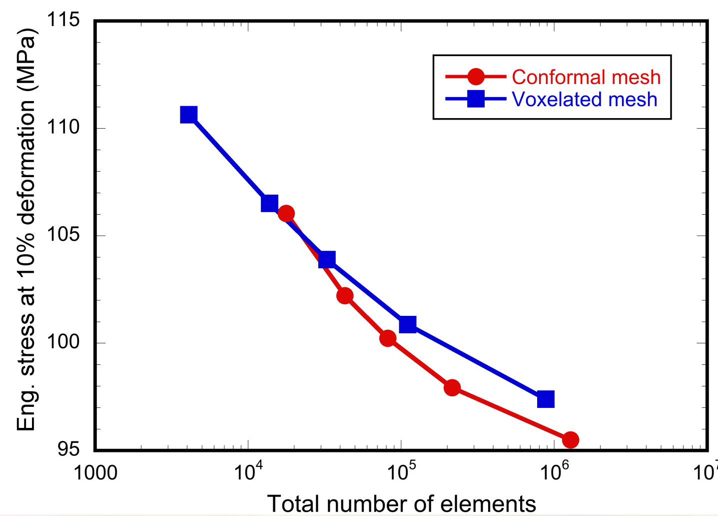

Stress Distributions at 10% Deformation

Uniaxial tension 10%

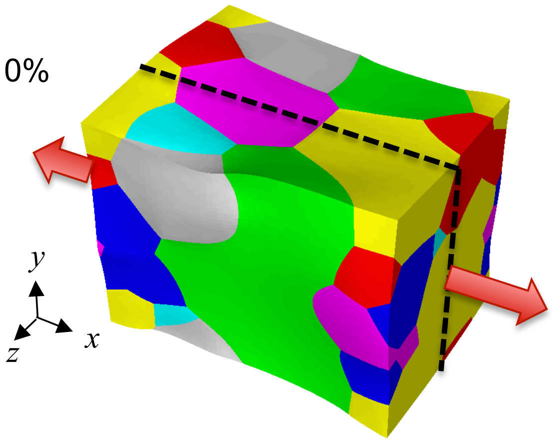

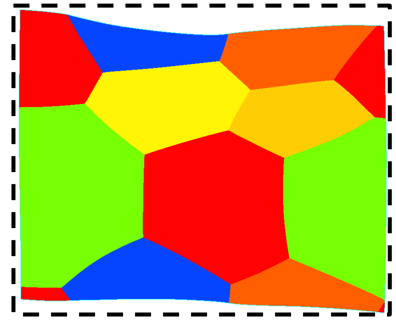

Voxelated mesh

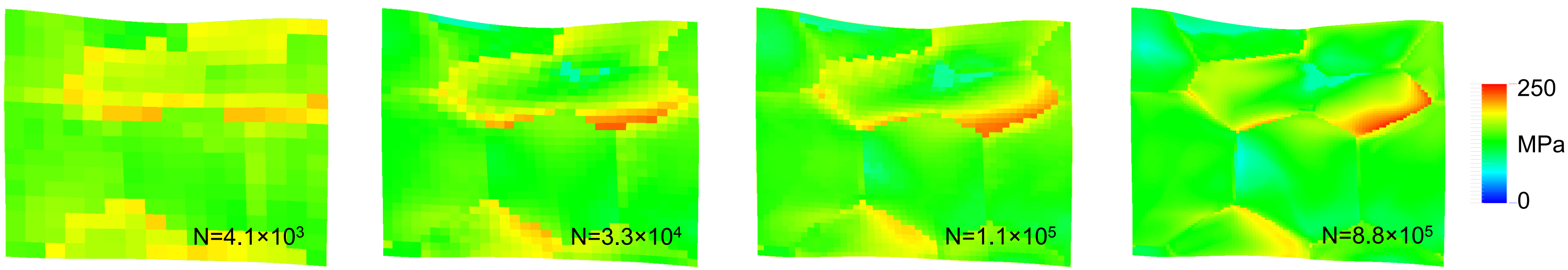

Conformal mesh

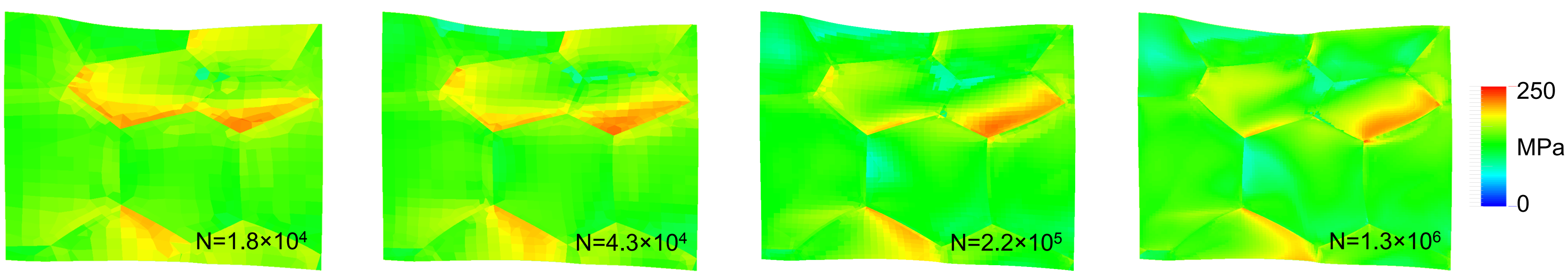

Further application of the technique

Laser weld on SS 304 L

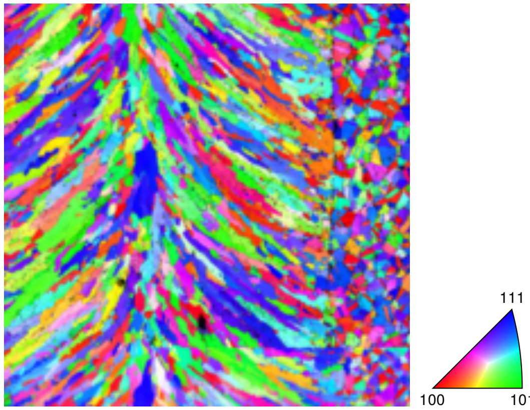

EBSD

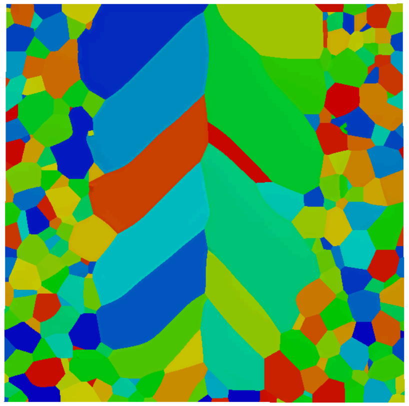

SPPARKS

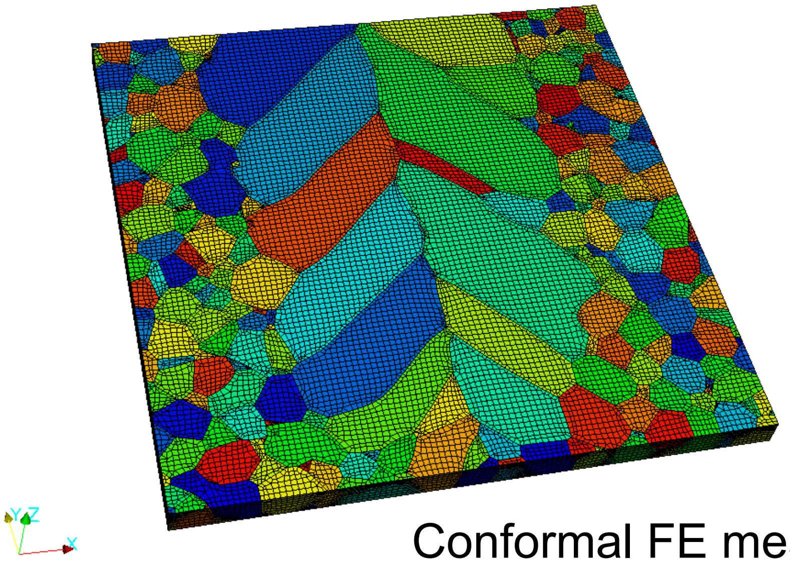

Conformal FE mesh

Monte Carlo Potts Simulations

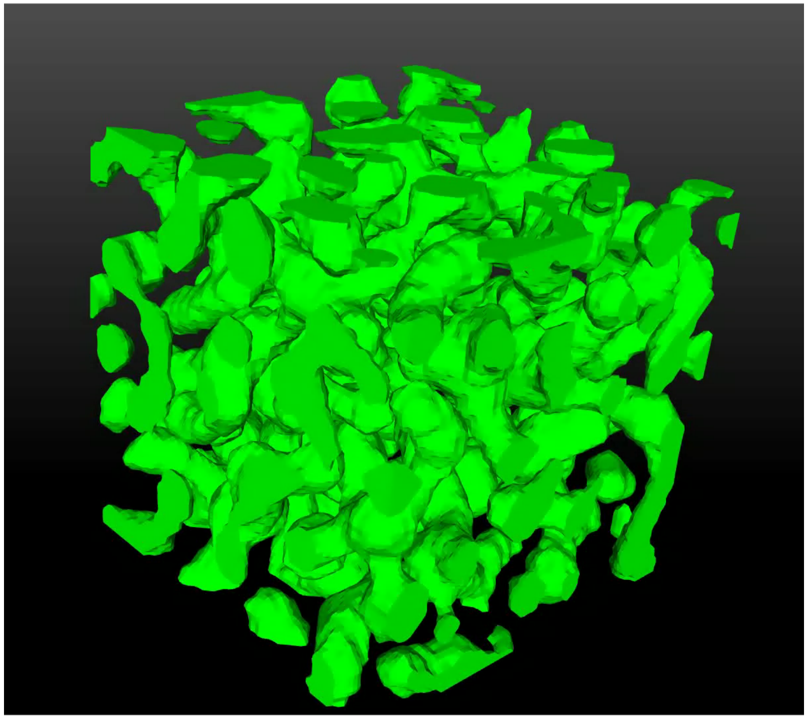

Summary

- Developed T and $\dot{\varepsilon}$ dependent flow rule based on dislocation kink-pair theory for Mo, Ta, W and Nb.
- CP-FEM predictions showed good agreement with experiments (HR-DIC, profilometry and EBSD) and capture grain-scale variability in mechanical responses.
- Developed conformal, hexahedral finite element meshing technology for three-dimensional polycrystalline microstructures
- Proposed computational method provides a convenient and direct link from the fundamental dislocation physics to the continuum-scale plastic deformation of Ta at the grain scale.

Thank you!

Acknowledgements
Predicting **P**erformance **M**argins (PPM)
Campaign **2** (C2) Dynamic Materials Properties
Advanced **S**imulation and **C**omputing – **P**hysics and **E**ngineering **M**odels (ASC-P & EM)